The techniques of surface alignment of liquid crystals

Greta Babakhanova[1,2], Oleg D. Lavrentovich[1,2,3]

[1] Advanced Materials and Liquid Crystal Institute, Kent State University, Kent, OH 44242, gbabakha@kent.edu, olavrent@kent.edu

[2] Chemical Physics Interdisciplinary Program, Kent State University, Kent, OH 44242

[3] Department of Physics, Kent State University, Kent, OH 44242

Contents

Introduction

Alignment of liquid crystal (LC) molecules is an important topic of physics of anisotropic fluids. The boundary conditions and the surface properties of the material in contact with an LC dictate the preferred orientation of the molecules at the interface. Several factors that affect the LC alignment include dipolar interactions, chemical bonding, van der Waals interactions, steric factors and surface topographies (Kahn et al. 1973; Lee 2014).

There are three main types of director alignment: planar, tilted, and homeotropic (or perpendicular). The nomenclature reflects how the director $\hat{\mathbf{n}}$ that specifies the average molecular orientation of the LC is aligned at the surface, Figure 1. In the planar case, $\hat{\mathbf{n}}$ is parallel to a single direction in the plane of the interface, so that the polar angle θ between the normal to the interface and $\hat{\mathbf{n}}$ is 90° and there is a well-defined direction in the plane, specified by some azimuthal angle φ, Figure 1. A degenerate case, when $\hat{\mathbf{n}}$ is free to be along any direction in the plane, so that φ is not fixed, is called a tangential alignment. Tilted alignment $0<\theta<90^{\circ}$ can be along a single direction or conically degenerate. In the homeotropic alignment, $\hat{\mathbf{n}}$ is perpendicular to the interface, $\theta=0$. Numerous techniques have been employed to align rod-like calamitic LCs (Cognard 1982). The challenge, however, is to align LCs with

molecules of complex shapes, such as bent-core and flexible dimer molecules, for which alignment is not always trivial (Iglesias et al. 2011; Elamain et al. 2013). Orienting water-based lyotropic LC systems is also difficult, but it is of great significance as this class of materials is often biocompatible. The stability of the alignment is one of the essential factors when assessing proposed methods, as environmental factors such as temperature, light polarization or humidity often affect the desired orientation. Though LCs are predominantly used in display technologies, the trend has now shifted towards biological application. Reports on LC alignment methods are vast. Therefore, in this chapter, we aim to briefly overview some of the widely used effective alignment approaches, report on the recently developed methods and extend on alignment techniques for non-calamitic LCs with molecules of complex shape. We conclude with discussing the advances, challenges and significance of using ordered, anisotropic LCs as templates for guiding biological matter.

Planar alignment

Below we discuss the most popular approaches to planar alignment and tilted alignment with a small "pretilt" angle, measured as $\alpha = 90^{\circ} - \theta$, $0 < \alpha < 10^{\circ}$.

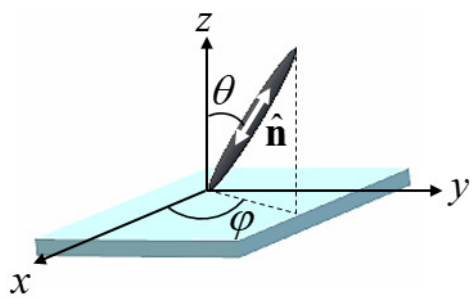

Figure 1. Schematic representation of LC molecule depicting the polar (θ) and the azimuthal (φ) angles.

Grooved surfaces

One mechanism of alignment proposed by Berreman is based primarily on geometrical factors that arise from elastic energy if the surface in contact with LC is grooved (Berreman 1972, 1973). There are many methods that can be implemented to produce grooved surface topography, which include rubbing/polishing the substrate, deposition of material by evaporation, ion beam etching and lithographic techniques. Berreman considered the grooved surface as a sinusoidal wave $z \approx A \sin qx$ defined with an amplitude A and wavelength $\lambda = \frac{2\pi}{q}$ (Figure 2) (Berreman 1972).

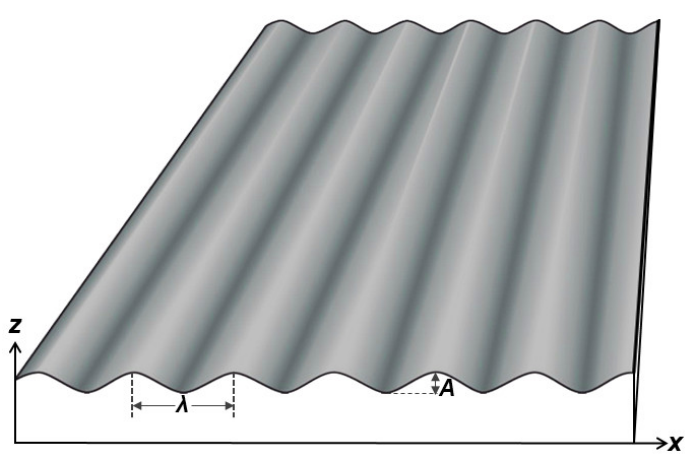

Figure 2. Schematic representation of a sinusoidal grooved surface.

Theoretical calculations of elastic energy of a liquid crystal in contact with such a substrate, assuming that the director is always tangential to the modulated surface and is aligned along a certain azimuthal direction φ, leads to the following elastic energy per unit area

$$F_{\mathrm{d}} = \frac{K}{4} A^2 q^3 \cos^2 \varphi, \qquad (1)$$

where K is the elastic constant of the LC in the so-called one-constant approximation. As clear from Eq.(1), the equilibrium alignment of $\hat{\mathbf{n}}$ is along the grooves, i.e., along the *y*-axis in Figure 2, as this is the only direction of alignment that causes no elastic distortions of the LC.

Deposition of polymeric coating

A typical LC cell is comprised of two sandwiched glass plates separated by spacers. Prior the assembly, the inner side of each glass plate is treated with an aligning agent, such as a thin polymer layer, to induce the desired LC director orientation (Cognard 1982; Geary et al. 1987). Appropriate polymer coatings such as polyimides (PIs) are optically transparent, stable and can withstand relatively high temperatures $(> 200°\mathrm{C})$. The PI coating alone yields tangential anchoring of LCs, however, rubbing it with a velvet cloth, for example, will cause the rubbed surface to become unidirectionally anisotropic (Lee et al. 1996). Thus, rubbed PI layer induces a preferred azimuthal direction of LCs (Chen 2016). Van Aerle explored the degree of orientation of the rubbed polymer layer in terms of Hermans' orientation factor f and determined that $0.5 < f < 1$, which indicates that rubbing process is an effective way to induce molecular orientation of a polymer layer (van Aerle and Tol 1994). Table 1 lists commercially available PI layers that produce the indicated pretilt angles (Takatoh 2005).

Rubbing generates grooves and scratches on the polymer surface (Zhu et al. 1994). On that account, some suggest that surface topography may cause long-range elastic effects and orient the long axes of LC molecules in the grooves parallel to the rubbing direction, as in the Berreman's model (Berreman 1972, 1973; Lee et al. 1993; Zhu et al. 1994). Another plausible mechanism is reorientation of polymer chains during rubbing (Castellano 1983; Geary et al. 1987; Vanaerle et al. 1993; Murata et al. 1993; van Aerle and Tol 1994; Toney et al. 1995; Lee et al. 1996; Lee et al. 1997). X-Ray scattering measurements demonstrate that rubbing a PI film causes near surface alignment of the polymer molecules parallel to the rubbing direction (Toney et al. 1995). Buffing-induced birefringence measurements by Geary et al and the Langmuir-Blodgett aligning films (nonrubbed) developed by Murata et al also show that the orientation of polymer molecules is the primary driving mechanism of the LC alignment, and not the nanogrooves (Geary et al. 1987; Murata et al. 1993).

The schematic representation of the rubbing process and generated molecular reorientation of polymer chains is illustrated in Figure 3. Intermolecular forces between the polymer and LC molecules are of great importance in aligning such buffed system and favor parallel alignment (Kleman and Lavrentovich 2003; Yang and Wu 2014). Even though rubbing PI layers results in good alignment of rod-like and bent shape LC molecules, a significant shortcoming of this technique is the accumulation of static charges and formation of fine dust particles which may deteriorate performance of LC displays (Lee 2014).

The strength of alignment is determined by using anchoring energy concept (de Gennes and Prost 1995). The anchoring energy, $W(\theta,\varphi)$, is defined as a measure of work per unit area needed to deviate the director from the so-called "easy axis" (θ_0,φ_0) that corresponds to the director orientation that sets the minimum of the surface energy: $W = \frac{1}{2} W_\theta \left(\theta - \theta_0\right)^2$ or $W = \frac{1}{2} W_\varphi \left(\varphi - \varphi_0\right)^2$, where W_θ and W_φ is the polar and azimuthal anchoring coefficients. For small director deviations from the easy axis, the surface anchoring potential for tangentially anchored substrates may be approximated by Rapini-Papoular expression (Rapini and Papoular 1969):

$$W = \frac{1}{2} W_\theta \sin^2\left(\theta - \theta_0\right) + \frac{1}{2} W_\varphi \sin^2\left(\varphi - \varphi_0\right). \qquad (2)$$

Anchoring strength is considered weak, when W : $\left(10^{-7} - 10^{-5}\right)$ J/m^2 and strong, when W : 10^{-3} J/m^2; typically, $W_\theta > W_\varphi$ by one or two orders of magnitude (Blinov and Chigrinov 1994; Kleman and Lavrentovich 2003; Yang and Wu 2014; Muševič 2017).

Table 1. Commercially available polyimide alignment materials that generally yield planar alignment for conventional rod-like liquid crystals (Takatoh 2005).

Name	Pretilt angle	Manufacturer	Name	Pretilt angle	Manufacturer
AL1454	0.7˚	JSR	AL1J508	4.7˚	JSR
LQ-2200	0.8˚	Hitachi Chem. Dupont	SE-150	4-5˚	Nissan Chem. Corp.
JALS-146-R39	1˚	JSR	SE-3310	4-5˚	Nissan Chem. Corp.
AL5056	2˚	JSR	SE7992	4-5˚	Nissan Chem. Corp.
SE2555	2˚	Nissan Chemicals Corp.	JALS-1024-R1	4-5˚	JSR
SE-410	2˚	Nissan Chemicals Corp.	JALS-9800-R1	4-5˚	JSR
SE-130	2˚	Nissan Chemicals Corp.	JALS-1077-R2	5˚	JSR
SE-2170	2˚	Nissan Chemicals Corp.	SE3140	5-6˚	Nissan Chem. Corp.
LX-1400	2.6˚	Hitachi Chem. Dupont	SE5291	5-6˚	Nissan Chem. Corp.
AL8254	3˚	JSR	JALS-9005-R1	5-6˚	JSR
LQ-C100	3.1˚	Hitachi Chem. Dupont	SE7492	6-7˚	Nissan Chem. Corp.
AL3408	3-4˚	JSR	LQ-T120-04	6.8˚	Hitachi Chem. Dupont
AL3046	3.5˚	JSR	SE-610	7-8˚	Nissan Chem. Corp.
LQ-T120-03	3.5˚	Hitachi Chem. Dupont	SE3510	7-8˚	Nissan Chem. Corp.
JALS-1068-R2	4.3˚	JSR	LQ-1800	8.0˚	Hitachi Chem. Dupont
AL1F408	4.5˚	JSR			

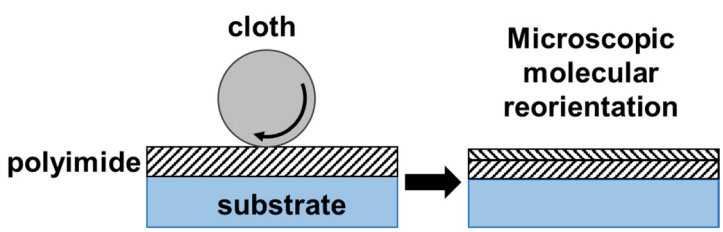

Figure 3. Schematic diagram of polyimide rubbing process resulting in microscopic molecular reorientation. Adapted with permission from Lee KW, Paek SH, Lien A, Durning C, Fukuro H (1996) Microscopic molecular reorientation of alignment layer polymer surfaces induced by rubbing and its effects on LC pretilt angles. Macromolecules 29 (27):8894-8899. Copyright (1996) American Chemical Society.

Carbon nanotube films

Carbon nanotubes (CNTs) are hollow cylindrical molecules which consist of rolled sheet of single-layer carbon atoms. Their aspect ratios may reach up to : 10^7, owing to their nanometer diameter and length that may extend up to centimeters (Ren et al. 2013). CNTs are a subject of intense research due to their extraordinary physical properties such as high tensile strength, high electrical and thermal conductivities, high ductility, high chemical and thermal stability (Ren et al. 2013). CNTs also exhibit anisotropic physical properties (Ren et al. 2013).

Single-layer CNT sheets have attracted a lot of interest, since these highly optical transparent coatings may simultaneously serve as both a LC alignment layer and a conductive layer (Russell et al. 2006; Fu et al. 2010; Rahman et al. 2018; Truong et al. 2019). Single-layer sheet can be drawn continuously from a vertically grown CNT forest, which facilitates mass production of these sheets at a commercial level (Truong et al. 2019). Russell et al generated

aligned single-walled CNT films via self-assembly as well as dip-coating methods and achieved uniform planar alignment of nematic LCs on the scale of centimeters (Russell et al. 2006). Their inherent conductive property eliminates the need of additional costly transparent electrodes for electro-optical applications. The surface topography of aligned CNTs observed via atomic force microscopy shows parallel grooved structures with an amplitude on the order of : 10^2 nm, much larger than grooves resulted from rubbed PI layers described in the previous section (Fu et al. 2010; Truong et al. 2019). It is proposed that since the long-chain structure at the surface does not exist, the mechanism of LC alignment is realized via grooved surface roughness of unidirectionally aligned CNTs (Russell et al. 2006; Fu et al. 2010).

CNTs are attractive aligning materials because they may be implemented in flexible/foldable electro-optical systems (Rahman et al. 2018). The current issue which is being addressed is the difficulty of attaining good adhesion between CNTs and substrate while keeping the orientational order as high as possible (Rahman et al. 2018). Truong and co-workers have recently explored this issue and reported that the hydrophobic treatment of the substrate using hexamethyldisilazane prior to the deposition of CNT sheet improved the adhesion between aligned CNT bundles and the glass substrate (Truong et al. 2019). The authors also eliminated the problem of short-circuit failure of the sandwich LC cell due to floating CNT nanofibrils that unintentionally connect two facing CNT-sheet electrodes by depositing an alumina passivation layer (Truong et al. 2019).

Photoalignment

One of the most powerful alignment methods employs light-matter interaction to induce controlled LC alignment. Contact-free photoinduced alignment technique eliminates undesired contaminants such as electrostatic charges, impurities as well as mechanical damage of the surface which may be caused by conventional rubbing of PI films (Ichimura et al. 1988; Gibbons et al. 1991; Schadt et al. 1992; Dyadyusha et al. 1992; Chigrinov et al. 2008; Pasechnik et al. 2009). Some of the greatest assets of this method is the ability to achieve rewritable, complex and nonuniform spatial patterns of the director field on flat or curved substrates, which are otherwise impossible to realize (Presnyakov et al. 2005). Additionally, photoalignment systems have an ability to achieve nano-scale alignment (Shteyner et al. 2013). Photopatterning is widely used in LC display applications, however, recently this alignment method became extensively used to fabricate functional materials such as stimuli-responsive films/coatings (Figure 4), sorting systems and optical elements (Slussarenko et al. 2011; McConney et al. 2013; Gao et al. 2015; White and Broer 2015; Ware et al. 2015; Wai Tam et al. 2016; Peng et al. 2016a; Peng et al. 2017a; Babakhanova et al. 2018; Bushuyev et al. 2018).

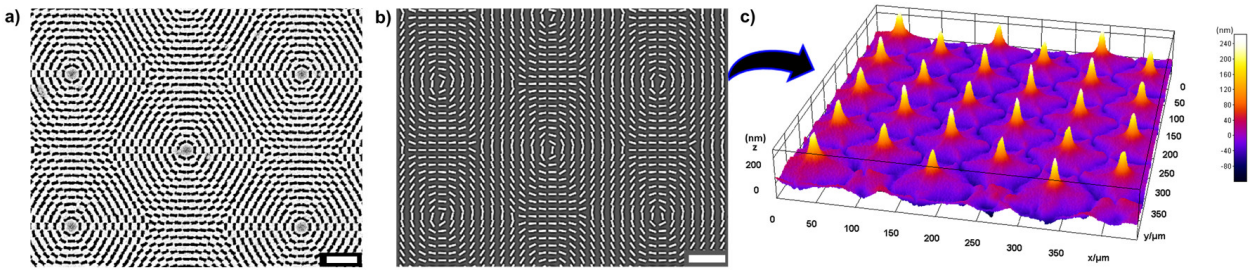

Figure 4. a) Scanning electron microscopy (Quanta 450) image of a plasmonic metamask made of nanoaperture arrays in Al film exhibiting an array of topological defects, (scale bar 1 µm), **b)** LC PolScope (Abrio Imaging Systems) image of the director field of a photopatterned liquid crystal elastomer coating that closely follows the nanoaperture orientations in the plasmonic metamask in panel **(a)**, (scale bar 50 µm), **c)** digital holographic microscopy (DHM) image of a photopatterned thermoresponsive liquid crystal elastomer coating at $T = 100\,°C$ forming nanometer surface profiles composed of hills/valleys in controlled locations preprogrammed by the director field orientation in **(a,b)**. Bend deformations shown in **(a,b)** result in hills illustrated in **(c)** as described in (Babakhanova et al. 2018).

One can distinguish at least four types of photoalignment mechanisms: 1) photochemically reversible *trans-cis* isomerization in materials containing azobenzene dyes, 2) reorientation of azo-dye chromophore molecules under the action of polarized light, 3) photodegradation and orientational bond breaking in polyimides, and 4) photochemical crosslinking in preferred directions of polymer precursors, such as cinnamoyl side-chain polymers (Chigrinov et al.

2005; Chigrinov et al. 2008; Yaroshchuk and Reznikov 2012). The first two mechanisms are reversible, whereas the other two processes involve irreversible photochemical changes (Chigrinov et al. 2008).

Azobenzene molecules have two conformations: *trans* and *cis* (Figure 5a), where the *trans* rod-like isomer is thermodynamically more stable than its bent (*cis*) counterpart (Aguilar and San Román 2014). Azobenzenes undergo reversible *trans-cis* isomerization when irradiated in their absorption bands (Bandara and Burdette 2012; Aguilar and San Román 2014). Usually, UV irradiation creates an excess of *cis*-isomers, while visible light converts most of the molecules into *trans* form. Ichimura and coworkers used azobenzene molecules attached to a substrate as a "commanding layer" of photoalignment: rod-like trans-isomers would align the adjacent LC molecules perpendicularly to the surface, while bent cis-isomers would support tangential alignment. The alignment can thus be switched by light driven isomerization from homeotropic to tangential and back (Figure 5b) (Ichimura et al. 1988). It is important to note that the degradation of the dye layer may impact the number of possible reversible cycles from *trans* to *cis* conformation.

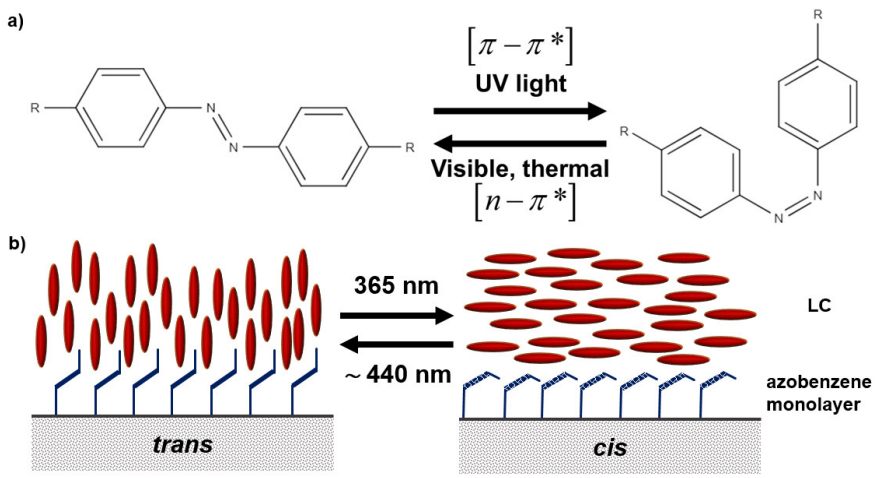

Figure 5. a) Schematic representation of an azobenzene unit that changes from trans conformation to cis upon illumination of UV light $(\lambda$=365 nm$)$, while visible light $(\lambda > 400$ nm$)$ restores the trans form, **b)** cartoon image of photoinduced homeotropic to planar alignments of LCs using trans-cis conformational changes of azo-dye moieties. Adapted with permission from Ichimura K, Suzuki Y, Seki T, Hosoki A, Aoki K (1988) Reversible Change in Alignment Mode of Nematic Liquid-Crystals Regulated Photochemically by Command Surfaces Modified with an Azobenzene Monolayer. Langmuir 4 (5):1214-1216. Copyright (1988) American Chemical Society.

The second photoalignment mechanism is the pure reorientation of azo-dye molecules due to polarized light (Kozenkov et al. 1986; Barnik et al. 1989). The azo-dyes strongly absorb light if the exciting optical field polarization is parallel to the dipole transition moment (Lee 2003). Azobenzenes in *trans* conformation with their transition moments parallel to the polarization direction of the incident light undergo reversible isomerization to *cis* state, where the probability of absorption is $\cos^2 \varsigma$; ς is the angle between the transition moment of an azobenzene and the linear polarization direction of the irradiating light (Li 2013; Aguilar and San Román 2014). Thus, the isomers whose transition moments are perpendicular to the linear polarized light have a very low probability of undergoing photoisomerization (Bandara and Burdette 2012). Photodriven alignment of azobenzene chromophores perpendicular to the UV light polarization, also known as Weigert effect, is realized as the net population of azobenzene moieties reorient perpendicularly to the linearly polarized light (Li 2013).

One of the recently developed methods utilizing pure azo-dye reorientation is the plasmonic photoalignment technique that utilizes plasmonic metamasks (PMMs). The PMM represents a thin Al film with an array of rectangular 100 nm x 220 nm nanoapertures (Figure 4a) (Guo et al. 2016). Unpolarized light transmitted through a PMM acquires linear polarization that is perpendicular to the long axis of the nanoapertures. Thus, a transmitted light with a pattern of both intensity and polarization is produced, which is then projected onto an azo-dye coated photosensitive materials that is previously spin-coated onto a glass substrate. Guo et al used Brilliant Yellow (BY) (Sigma Aldrich) and PAAD-72 (BeamCo) photoalignment materials (Guo et al. 2016). Once polarized light irradiates the azo-dye molecules, photochemical reaction is induced that results in the reorientation of their long axes perpendicularly to the local light polarization. When LC is in contact with prepatterned photoaligned coating, the director closely follows the orientation

inscribed into the alignment of dye molecules; in other words, the orientational pattern of the liquid crystal is the same as that one of nanoapertures in the PMM (see Figure 4b and Figure 4a) (Guo et al. 2016).

One of the major drawbacks of photoalignment using azo-dyes is the sensitivity of the photoalignment materials to humidity (Wang et al. 2017). Humidity may effect the wetting of the photoresponsive film during the spin-coating process (Hecht et al. 1998). Wang et al explored the effect of relative humidity (RH) levels at different stages of photoalignment preparation using dichroic azo-dye BY: at the stage of substrate storage before coating, during the spin-coating process, between film coating and exposure, and after exposure (Wang et al. 2017). The greatest effect of RH on the order parameter of the photoalignment layer was at the time of spin-coating process of the dimethylformamide/BY solution, the results in Figure 6 indicate that the best alignment is achieved at RH levels $<45\,\%$, and no alignment is achieved at RH levels $>50\,\%$ (Wang et al. 2017). The absorption spectra of the prepared BY films (prepared at different RH levels at the time of spin-coating) shows a red-shift with increase in RH, possibly, due to the change in BY aggregation (Wang et al. 2017). Grazing incidence X-ray diffraction patterns in the case of BY dispersed in triacetyl cellulose show that humidity triggers restructuring of the BY assembly from 1D nematic-like order to 2D rectangular lattice composed of columnar order of BY molecules, resulting in the dramatic increase in the order parameter (Matsumori et al. 2015). During the humidification process, hydration might occur site-selectively around the sodium sulfonate hydrophilic functional groups that may enhance the lyotropic liquid crystalline property of BY which facilitates the reordering of the molecules into columnar assemblies (Matsumori et al. 2015). Storing conditions before polarized light exposure also greatly effect the photoalignment. Wang et al show that unexposed BY films kept at high humidity $(80\text{-}90\%\,\mathrm{RH})$ for 2.5 hr show no alignment $(S\text{=}0.01\text{-}0.11)$, while films kept at moderate humidity $(40\text{-}45\%\,\mathrm{RH})$ show relatively constant order parameter $(S\text{=}0.76\text{-}0.79)$ (Wang et al. 2017). Thus RH levels need to be taken into consideration as humidity absorption plays an important part during the photopatterning process.

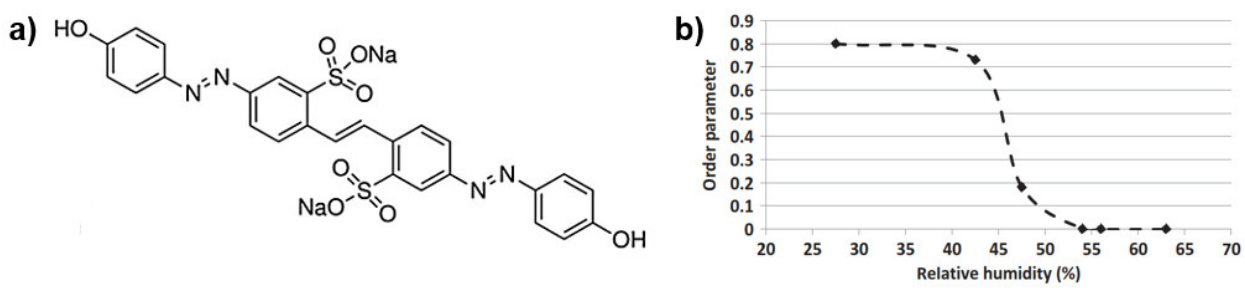

Figure 6. a) Azo-dye BY, **b)** Order parameter (S) as a function of relative humidity levels during the spin-coating photosensitive layer BY Reprinted by permission of the publisher Taylor & Francis Ltd., Wang JR, McGinty C, West J, Bryant D, Finnemeyer V, Reich R, Berry S, Clark H, Yaroshchuk O, Bos P (2017) Effects of humidity and surface on photoalignment of brilliant yellow. Liquid Crystals 44 (5):863-872.

Another photoinduced alignment mechanism involves breaking polyimide chains with UV light (Hasegawa 1999). Initially, the PI chains are randomly oriented in the plane of the film. Upon UV irradiation, the PI chains that are parallel to the UV polarization decompose. The remaining chains oriented perpendicular to the polarization of light remain intact. Thus, the direction of LC alignment due to van der Waals forces is parallel to the maximum density of unbroken polyimide chains (Chigrinov et al. 2008). One of the major limitation of photodegradation is the small value of the orientational order parameter, its accurate control and high sensitivity to UV exposure time (Figure 7) (Sung et al. 2001; Chigrinov et al. 2008). Additionally, the by-products may contaminate the system by reducing the thermal stability of the alignment layer, producing ions that may cause image sticking or flickers (Yang et al. 1996; Wang et al. 2001).

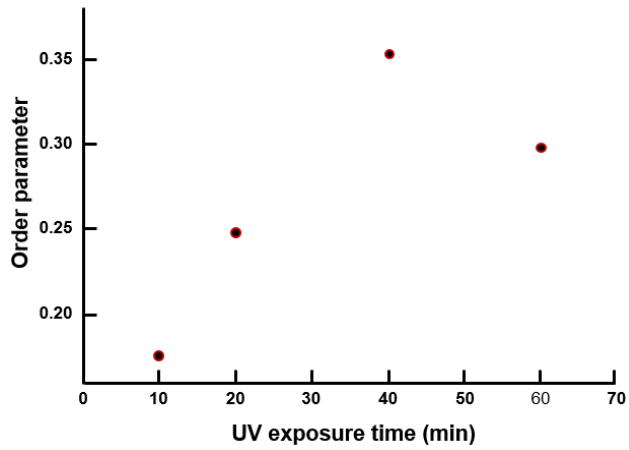

Figure 7. Order parameter of LC cells as a function of UV exposure time. Adapted from Sung SJ, Kim HT, Lee JW, Park JK. Photo-induced liquid crystal alignment on polyimide containing fluorine group. Synthetic Met 117 (1-3):277-279. Copyright (2001) Elsevier.

The photoalignment mechanism developed by Schadt and coworkers is based on a different class of photoresponsive materials (typically used as a negative photoresist), called polyvinyl 4-methoxy-cinnamate (PVMC) (Schadt et al. 1992). The UV irradiation causes a topochemical reaction between the side chains of prepolymer containing cinnamate (Chrzanowski M. M. 2011). The optical excitation of $\pi-$electrons in double-bonds of cinnamoyl moieties is polarization dependent (Schadt 2017). Thus, under linear photo-polymerization (LPP) the prepolymer undergoes [2+2] cycloaddition of cinnamic acid side chains that belong to different main chains, where parallel double bonds, one from each molecule, are broken and reform as single bonds between molecules (Figure 8, Figure 9) (Schadt et al. 1992; Ogawa and Kanemitsu 1995). LPP leads to a preferred depletion of cinnamic acid side chain along linearly polarized UV light $(\lambda = 320\ \text{nm})$. Consecutively, LPP causes anisotropic distribution of cyclobutane molecules with their long axis perpendicular to the polarization direction of the incident polarized UV light (Schadt et al. 1992; Chigrinov et al. 2008). When in contact with PVMC films, LCs align along the long axis of cyclobutane molecules due to van der Waals forces. LPP-photoalignment technology allows generation of pre-tilt angles ranging from $0° - 90°$ and simultaneously fixation of the alignment (Schadt et al. 1992). The major drawback of this technique is the low thermal stability.

Figure 8. [2+2] cycloaddition; a model for polymerization.

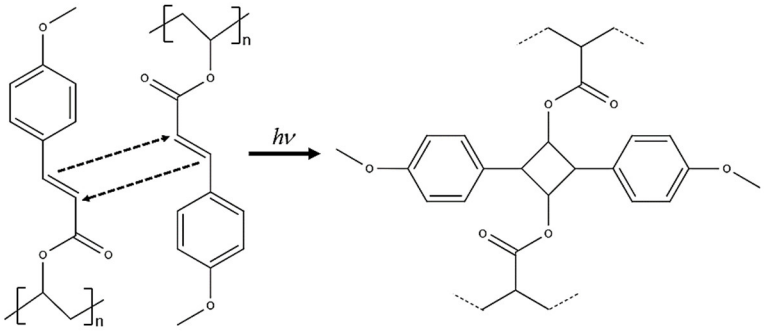

Figure 9. Two poly(vinyl 4-methoxycinnamate) side chains undergo intermolecular photo-induced [2+2] cycloaddition. Adapted from (Schadt et al. 1992).

There are other light-driven techniques that achieve LC alignment without involving any dyes. Scanning wave photopolymerization (SWaP) is a dye-free alignment method that does not require polarized light (Hisano et al. 2016; Hisano et al. 2017). SWaP allows to achieve arbitrary, complex 2D alignment patterns over large areas without any prior surface treatments with resolution down to $: 2\ \mu m$ (Hisano et al. 2017). SWaP uses spatiotemporal scanning of focused guided light and is triggered by mass flow in the film arising from molecular diffusion in the light intensity gradient as the polymerization reaction propagates (Hisano et al. 2017; Aizawa et al. 2018). This single step process results in LC alignment parallel to the incident light patterns. The limiting factor of SWaP is that it is currently applicable to aligning photopolymerizable LCs with thicknesses below tens of micrometers (Hisano et al. 2017).

Tilted alignment

Generally, buffed polymer main chains described in the earlier section result in small pretilt angles (see Table 1). The alkyl branches in a PI layer affect the magnitude of the pretilt angle. For example, in the absence of the alkyl branches, the pretilt is very small: $\alpha : 2°$, whereas low and high density of alkyl chains results in an increase of the tilt angle $(: 5° - 20°)$ (Pasechnik et al. 2009). Control of the tilt angle is crucial in applications in which there is a pre-requisite of molecular realignment along a single predetermined direction (Cognard 1982). In order to achieve relatively high pretilt $(: 30°)$, generally, an oblique evaporation of silicon oxides (SiO_x) is used (Janning 1972; Meyerhofer 1976). Depending on the angle between the substrate plane and the direction of the incident beam (Figure 10), tilt angles ranging from $0° - 90°$ may be obtained (Cognard 1982). The incident angle of evaporation (β) causes the film to "grow" in the preferred direction forming micro-columnar structures on the surface of the substrate via self-shadowing mechanism (Janning 1972; Skarp et al. 1988; Takatoh 2005; Lakhtakia and Messier 2005; Liou et al. 2006; Pelliccione and Lu 2008). When in contact with such a surface, LCs orient in the direction of the film growth (defined by the azimuthal angle of the evaporation direction) (Janning 1972). The features of the surface structures of the oblique evaporated film change with β (Takatoh 2005; Liou et al. 2006; Oton et al. 2014).

In order to achieve high in-plane uniformity of the film as well as high accuracy of the evaporation angle, the source must be placed at a large distance from the target substrate. The drawback of this technique is the cost of the vacuum equipment. Another considerable disadvantage is the need of large chambers to accommodate bigger substrates, which may pose a problem for high volume production.

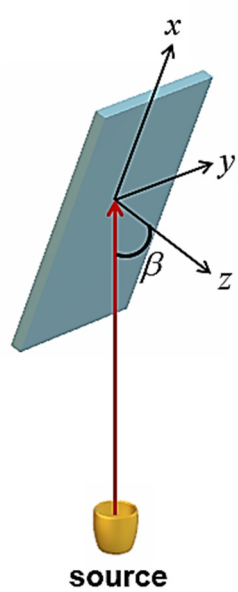

Figure 10. Schematic representation of oblique evaporation system, where *z*-axis represents the surface normal, β is an angle between the surface normal and the evaporation direction.

Alternatively, another approach to control the pretilt is to mix planar and homeotropic polyimides. The mixing ratio, baking temperature and rubbing strength influence the pretilt angle (Yeung et al. 2006a; Yeung et al. 2006b; Ho et al. 2007; Vaughn et al. 2007; Kim et al. 2007; Wu et al. 2008). This technique allows achieving pretilt angles ranging from $0° - 90°$, where the pretilt angle increases monotonically with the increasing concentration of homeotropic PI (Figure 11a) (Yeung et al. 2006a; Ho et al. 2007; Wu et al. 2008). The pretilt drops with the lower concentration of homeotropic PI due to the decline in the concentration of alkyl side chains associated with homeotropic PI (Vaughn et al. 2007). Increasing the baking temperature also results in monotonous decline of pretilt angle (Figure 11b). This observation is expected, since over-baking polyamic acids has two consequences: 1) it initiates imidization of the backbones of homeotropic PI promoting planar alignment, 2) cleaves away a fraction of the side chain of the homeotropic PI component which weakens the vertical alignment (Vaughn et al. 2007; Wu et al. 2008). Lastly, the pretilt may also be affected by the strength of rubbing the homeotropic PI (Figure 11c). When mixture of horizontal and vertical PIs is used, the tendency to align horizontally increases with increasing strength of rubbing, thus reducing the pretilt angle (Wu et al. 2008).

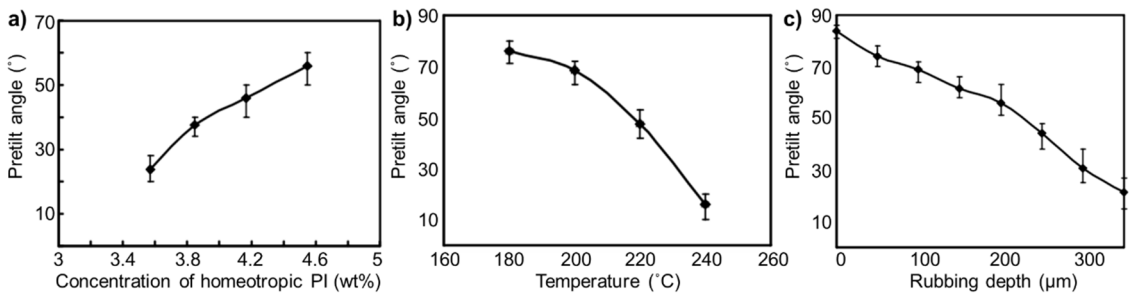

Figure 11. Variation of pretilt angle as a function of **a)** concentration of homeotropic PI in the mixture, **b)** baking temperature, **c)** rubbing strength. Adapted with permission from Wu WY, Wang CC, Fuh AYG (2008) Controlling pre-tilt angles of liquid crystal using mixed polyimide alignment layer. Opt Express 16 (21):17131-17137. © The Optical Society.

Vertical alignment

Vertical, or homeotropic, alignment generally refers to LC molecular orientation such that $\theta = 0°$, although for some applications (such as electro-optical switching of LCs) a pre-tilt angle $(80° < \alpha < 90°)$ might be essential. There is no single method of homeotropic alignment that would work for all LCs. Nevertheless, surfactants and homeotropic PIs are typically successful in aligning conventional rod-like molecules. Homeotropic alignment for nontrivial shape of LCs, however, is rather challenging. Realizing a durable homeotropic alignment is of great importance, since tilting of the uniaxial director due to anchoring transition in some cases might be misinterpreted as a biaxial nematic phase (Senyuk et al. 2010; Kim et al. 2014a; Kim et al. 2014b; Kim et al. 2015). Thus, we will introduce two alignment layers techniques which were successful in aligning rigid bent-core as well as flexible bent-core molecules.

Deposition of surfactant

Surfactants are amphiphilic surface-active agents that are comprised of two parts: hydrophilic head group and hydrophobic hydrocarbon chain. The head and the tail of an amphiphile interact very differently with a polar or nonpolar media. Examples of popular surfactants that are generally used in LC alignment are lecithin (derived from eggs), hexadecyl-trimethylammonium bromide (HMAB), stearic acid, cetyl trimethylammonium bromide (CTAB) or dimethyloctadecyl[3-(trimethoxysilyl)propyl]ammonium chloride (DMOAP) (Figure 12). Note here that the quality of the homeotropic alignment via surfactants is highly dependent on the substrate and LC composition. Generally, (especially when using DMOAP) the cleanliness of the substrate is extremely important, since any organic residuals may hinder the desired alignment. Cleaning the glass substrates with piranha solution is very effective in removing organic residuals (Zhou et al. 2017).

It is also worth mentioning that the longevity of the alignment layers using surfactants is less stable than hard-baked PI coatings, since the absorbed layer slowly dissolves in the LC, which may also affect the composition and properties of the system (Cognard 1982). Thus, checking the isotropic – LC phase transition may be a convenient way to detect contamination due to an alignment layer, as doping LCs with small amounts of non-mesogenic compounds

significantly alters the clearing points (by a few Kelvins) (Dierking 2003). Humidity and heat may also damage the alignment (Cognard 1990; Yoon et al. 2011).

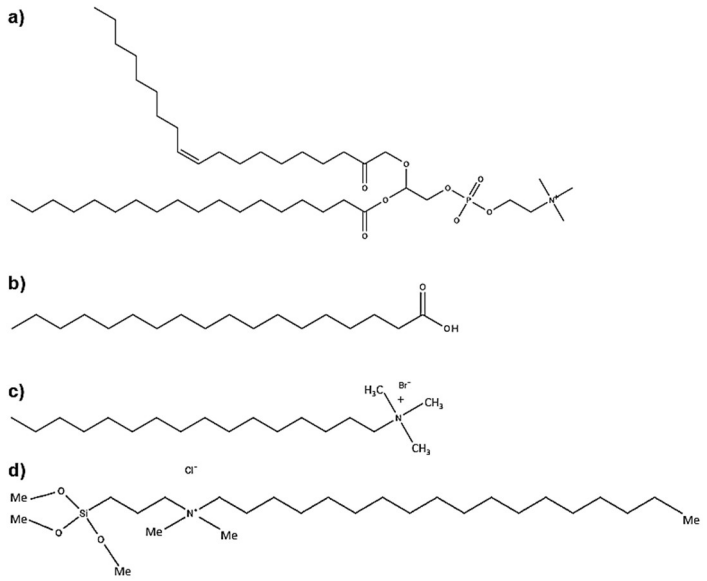

Figure 12. Conventional surfactants used for homeotropic alignment of LCs: **a)** lecithin, **b)** stearic acid, **c)** cetyl trimethylammonium bromide, **d)** dimethyloctadecyl[3-(trimethoxysilyl)propyl]ammonium chloride.

To set the homeotropic alignment using derivatives of lecithin, for example, clean glass substrates are typically treated with a weak solution of lecithin (0.1 - 2 wt%) in hexane by dipping or spin-coating methods. Dilution is important to avoid formation of unwanted spots (Cognard 1982). The excess amounts of lecithin may be washed out with the solvent, after which the substrates are dried for 30 min at 80 ˚C (Cognard 1982). The hydrophilic head groups attach to the substrate, extending their long hydrophobic alkyl chains perpendicular to the surface, forming brush-like structure (Hiltrop and Stegemeyer 1978).

The alignment properties of LCs on lecithin monolayers depend on the packing density (PD), where, generally, the orienting power of amphiphiles decreases with PD (Hiltrop and Stegemeyer 1978). One may precisely control PD by transferring a monomolecular layer of surfactants at the air-water interface onto a solid glass using Langmuir-Blodgett method (Roberts 1990). At proper concentrations, the alkyl brushes form elongated holes of molecular dimensions which can accommodate rod-like LC molecules (Hiltrop and Stegemeyer 1978). At low and high densities of alkyl chains, the steric interactions are not sufficient to induce homeotropic alignment, which results in random alignment. The model of steric interaction between surfactant layer and LC molecules that promotes vertical alignment proposed by Hiltrop et al is shown in Figure 13.

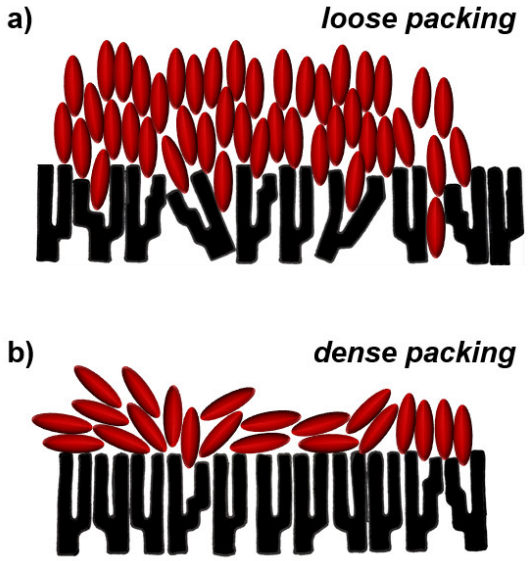

Figure 13. Schematic representation of the model of interaction between nematic LCs and lecithin monolayer: **a)** homeotropic alignment at low packing density, **b)** lack of anchoring at high packing density resulting in distorted alignment. Adapted from Hiltrop K, Stegemeyer H (1978) Alignment of Liquid Crystals by Amphiphilic Monolayers. Berichte der Bunsengesellschaft für physikalische Chemie 82 (9):884-889. Copyright (1978) Wiley-VCH and Bunsengesellschaft.

Homeotropic polyimide layers

Polyimides are generally mixed with a solvent, and the mixture is spin-coated onto a clean glass substrate to form a nano-layer coating (Armitage et al. 2006). The soft film then follows soft- and hard-baking procedures to generate a hard alignment layer. Each PI aligning agent has a unique curing temperature, though, generally the operational temperatures are very high to induce thermal imidization reaction (for example T_{curing} of the widely used SE-1211 and SE-7511L is 180 °C) (Armitage et al. 2006). The chemical structure of the homeotropic PIs is generally of side chain type, since the conventional rod-like LCs tend to align parallel to the side chain of the polymer (Hwang et al. 2003; Oh-e et al. 2004; Takatoh 2005; Park et al. 2007; Lee et al. 2007; Fang et al. 2010). Typically, rubbing homeotropic PIs is also employed to generate a pre-tilt angle as the side chain tends to align towards the rubbing direction. Rubbing has to be extremely delicate, since a single rubbing-induced scratch in a projection display may be easily observed when the image is magnified by : $50-100\times$ (Armitage et al. 2006).

Table 2. Commercially available polyimide alignment materials that usually yield homeotropic alignment (Takatoh 2005).

Name	Pretilt angle	Manufacturer
SE-1211	90°	Nissan Chemicals Corp.
SE-5661	90 °	Nissan Chemicals Corp.
SE-7511L	90°	Nissan Chemicals Corp.
JALS-682-R6	88°	JSR
JALS-2021-R2	89°	JSR
JALS-2022-R2	82°	JSR
JALS-204	89°	JSR

Rigid bent-core LCs

Note that the polyimide materials listed in Table 2 fail to produce homeotropic alignment of nematics formed by molecules of nontrivial shape, where Schlieren texture is observed instead (Kim et al. 2014b; Kim et al. 2016b). To stabilize the vertical alignment, a small amount of UV-curable reactive mesogen (RM) may be mixed with the homeotropic polyimide alignment layer (Lee 2009; Senyuk et al. 2011; Kim et al. 2014b; Kim et al. 2016b). For instance, rigid oxadiazole bent-core mesogens, which could not be aligned via SE-1211, SE-7511, and SE-5661, were successfully aligned homeotropically using RM-doping technique following the procedure below (Kim et al. 2016b):

The reactive mesogen RM-257 (Merck) was added to the polyimide SE5661 in a 1:50 weight proportion. A small amount (0.1 in weight proportion) of photoinitiator, Irgacure 651 (Ciba Chemicals), was then added. The mixture was spin coated on glass substrates and baked at $T = 170\,°\mathrm{C}$ for one hour. Subsequently, RM-SE5661 coated substrates were exposed to UV irradiation using 6 W UV $(\lambda = 365\,\mathrm{nm})$ lamp for 90 min to polymerize the reactive mesogens (Kim et al. 2016b). Such aligning protocol was used to achieve stable homeotropic alignment and establish the uniaxial nematic nature of the oxadiazole bent-core mesogens on the macroscopic scale. Similar approaches employed different aligning layers mixed with RMs to achieve high-performance homeotropic alignment (Lee 2009; Lee et al. 2013; Son et al. 2017).

Flexible bent-core LCs

Recently, flexible bent-core molecules were demonstrated in transmission electron microscopy studies to form a new nematic phase, called twist-bend nematic (Borshch et al. 2013; Chen et al. 2013). The reports on unusual behavior of material properties found new applications in electro-optics (Cestari et al. 2011; Adlem et al. 2013; Xiang et al. 2014a; Xiang et al. 2014b; Robles-Hernandez et al. 2015; Yun et al. 2015; Xiang et al. 2015; Lopez et al. 2016; Sebastian et al. 2016; Robles-Hernandez et al. 2016; Babakhanova et al. 2017; Cukrov et al. 2017; Sebastian et al. 2017; Iadlovska et al. 2018). The characterization of material parameters such as dielectric anisotropy and elastic constants requires one to prepare both planar and homeotropic alignment. Planar alignment (Figure 14a) is easily achieved with conventional methods of PI deposition (such as PI2555 in Table 1). Thus far, the homeotropic alignment, however, was only achieved for fluorinated flexible dimeric mesogens with negative dielectric anisotropy (Borshch et al. 2013; Cukrov et al. 2017; Jakli et al. 2018). The deposition of conventional PIs or surfactants alone either results in characteristic misaligned Schlieren texture or weak homeotropic alignment stable for only few degrees, as upon cooling, LC experiences anchoring transition and homeotropic alignment is lost. A stable homeotropic alignment was achieved using DMOAP-SE5661 double-layer deposition method outlined below (Cukrov et al. 2017).

To realize stable homeotropic alignment of fluorinated dimers (Figure 14b), first, the ITO-coated glass was cleaned in the ultrasonic bath, rinsed in deionized (DI) water and rinsed again with an Isopropyl Alcohol (IPA). To evaporate the solvent, the substrates were placed in an oven. After drying, the ITO glass was treated with UV ozone for 15 minutes. Subsequently, the substrates were immersed and agitated in 1 wt% aqueous solution of Dimethyloctadecyl[3-(trimethoxysilyl)propyl]ammonium chloride (DMOAP) (Sigma-Aldrich) for 25 minutes. The substrates were than rinsed with DI water for three minutes, dried with Nitrogen gas and cured in an oven at $T = 110\,°\mathrm{C}$. Lastly, the second alignment layer, SE5661 mixed with a thinner, Solvent 79, with 1:1 ratio (Nissan Chemical Industries), was spin-coated at 500 rpm (3 sec), 3000 rpm (30 sec), 50 rpm (1 sec) on ITO substrates. After the spin-coating procedure, the substrates were soft-baked at $T = 80\,°\mathrm{C}$ for 10 minutes, and, finally, baked at $T = 180\,°\mathrm{C}$ for 55 minutes (Cukrov et al. 2017). This procedure, however, does not align widely-used cyanobiphenyl-based flexible dimers. Therefore, further investigations will need to expand on alignment of other families of flexible dimers.

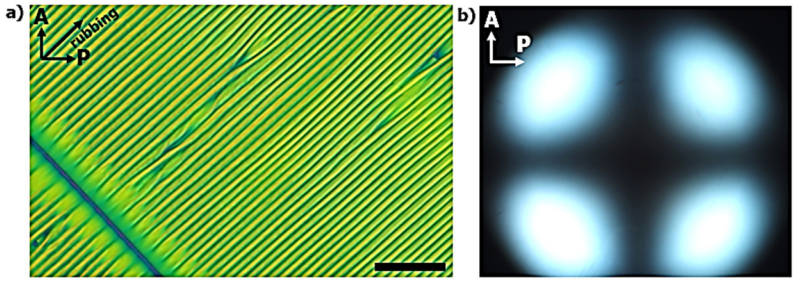

Figure 14. Polarizing optical microscopy texture of **a)** twist-bend nematic phase of 1,11-bis(2',3'-difluoro-4"-pentyl-[1,1':4',1"-terphenyl]-4-yl)undecane (DTC5C11) in a homogeneous planar cell treated by PI2555 polyimide layer with characteristic striped texture oriented along the rubbing direction at 45 degrees; **b)** conoscopy pattern characteristic of a homeotropic uniaxial nematic; the glass substrates of the homeotropic cell were treated with DMOAP-SE5661 dual alignment layer. Scale bar $50\ \mu m$.

Electric/Magnetic fields

Liquid crystals are highly susceptible to external fields. In this section, we will focus our discussion only on employing electric and magnetic fields as means to realign the director field. The reorientation of the director field occurs due to anisotropic LC electric polarization or magnetization. Under an applied external field and set boundary conditions at the boundaries that confine LCs, the equilibrium state of the director field will minimize the total free energy of the system (F) (Yang and Wu 2015). In case of an applied electric field, the mesogens with positive dielectric anisotropy $(\Delta\varepsilon > 0)$ orient along the electric field $(\mathbf{E})$ direction, while LCs with $\Delta\varepsilon < 0$ align perpendicular to $\mathbf{E}$. The reorientation from uniform configuration to deformed state of the director is called the Frederiks effect. The distortion of the director field occurs only above a certain threshold electric field (E_{th}) which overcomes the surface anchoring and the elasticity of nematic bulk defined as

$$E_{\text{th}} = \frac{\pi}{d}\sqrt{\frac{K_{\text{ii}}}{\varepsilon_{\text{o}}\left|\Delta\varepsilon\right|}}\ , \qquad (7)$$

where d is the thickness of a LC cell, K_{ii} is the splay, twist or bend elastic constant of LC, ε_{o} is the permittivity of free space, and $\Delta\varepsilon$ is the dielectric anisotropy of LC (Blinov and Chigrinov 1994). When the field is removed, surface anchoring restores the system to its original state (Kleman and Lavrentovich 2003). Note that Equation 7 is applied to a system with an assumption that the anchoring is infinitely strong. However, if the anchoring is weak, the director at the surface has a certain freedom to turn under the action of the elastic torque from the bulk (Blinov 2010). Consequetly, one needs to substitute d with $(d+2b)$, where $b = K_{\text{ii}} / W^{\text{s}}$ is the surface extrapolation length, where W^{s} is the surface anchoring energy (Blinov 2010). The schematic representation of cells filled with a LC with $\Delta\varepsilon > 0$ in three different geometries is presented in Figure 15, where Frederiks transition above E_{th} induces splay, twist and bend deformations of the director field.

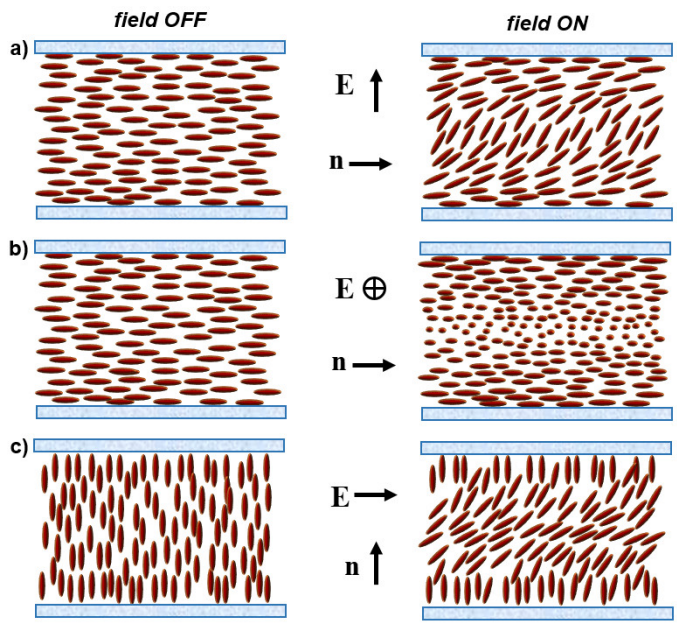

Figure 15. Schematic representation of three different geometries of Frederiks effect inducing **a)** splay, **b)** twist or **c)** bend deformations in a material with positive dielectric anisotropy which aligns parallel to the applied electric field. (Adapted by permission from Springer Nature: Soft Matter Physics. An Introduction by Kleman, M., Lavrentovich, O.D., Copyright (2003) Springer.

An application of magnetic field $(\mathbf{B})$ is analogous, where LCs with positive diamagnetic anisotropy $(\Delta\chi > 0)$ align parallel to applied $\mathbf{B}$, whereas LC with $\Delta\chi < 0$ align perpendicularly to $\mathbf{B}$. The threshold magnetic field is given by (Blinov and Chigrinov 1994; Kleman and Lavrentovich 2003)

$$B_{\text{th}} = \frac{\pi}{d}\sqrt{\frac{\mu_{\text{o}} K_{\text{ii}}}{\Delta\chi}}\,, \qquad (8)$$

where $\mu_{\text{o}} = 4\pi \times 10^{-7}\ \text{H m}^{-1}$ is the magnetic permeability of vacuum.

Electric or magnetic field may be employed to 1) aligned an initially unaligned director field, or 2) realign a well aligned director configuration as in Figure 15. The latter is the basis of many LC-based electro-optical applications. Commercial LC display companies exploit different switching modes (such as hybrid aligned nematic, vertical alignment, $\pi-$cell) by controlling the alignment at the boundaries of an LC-cell. Various modes yield different switching times, dark states, viewing-angle or contrast ratio (Lee 2014).

Aligned LCs as templates for guiding biological matter

For decades LC alignment was primarily used for display applications. Yet, other fascinating interdisciplinary developments also emerge that use anisotropic nature of LC, molecular ordering and sensitivity to external factors to design sophisticated functional devices. For instance, it was demonstrated that LC-based constructs may be efficiently employed as an optical amplification medium, as well as chemical or biological sensors (Gupta et al. 1998; Brake et al. 2003; Fang et al. 2003; Shiyanovskii et al. 2005; Kim et al. 2005; McCamley et al. 2007; Hunter 2012; Carlton et al. 2013; Popov et al. 2018; Kim et al. 2018). In particular, macroscopic detection of the "adsorbate-induced anchoring transition" can be confirmed by observing the textural changes of the LC-based sensor (Brake et al. 2003). This phenomenon occurs when amphiphiles adsorb to and alter the orientation ordering of LCs at aqueous-LC interfaces which changes the LC anchoring energy, where a coverage of the interface by adsorbate of 0.1 to 1 Langmuir (for example at least : 10 μg/ml solution concentrations of lipids) is usually required to change W to induce ordering

transition (Lin et al. 2011; Miller et al. 2014). Another example of an antibody-antigen binding detection/amplification in the *bulk* was demonstrated using water-based lyotropic chromonic LC (LCLC) medium, where the immune complexes larger than R_c are detected optically due to director distortions around them, while individual antibodies that are too small to perturb $\hat{\mathbf{n}}$ remain unseen (Shiyanovskii et al. 2005). The balance of two energies, KR and $W_\theta R^2$ dictate the behavior of the system, as the small inclusions that are not recognized by antibodies, of a size below $R_c < \frac{K}{W_\theta}$, do not distort the director field, whereas the antigen-antibody biding that creates bigger aggregates of targeted microbes distorts LCLC and produces optical signal once $R_c > \frac{K}{W_\theta}$ condition is satisfied.

There is a growing interest in LCLCs due to their biocompatibility (Mushenheim et al. 2014a; Zhou et al. 2014; Mushenheim et al. 2014b; Mushenheim et al. 2015; Peng et al. 2016b; Kumar and Pattanayek 2016; Zhou et al. 2017; Theis et al. 2018; Woolverton et al. 2005). Chromonic molecules self-assemble into ordered structures through weak, noncovalent interactions ($\pi - \pi$ attraction), depending on factors such as ionic content, pH, temperature, concentration, and molecular structure (Park 2012). The approaches to align LCLCs include rubbing glass, PI/graphene/silicon oxide deposition, photopatterning, micro-channel confinement, application of magnetic field, nanopatterning polymer films or self-assembling monolayers (Rapp et al. 1999; Lavrentovich and Ishikawa 2002; Fujiwara and Ichimura 2002; Ichimura et al. 2002; Ruslim et al. 2004; Nastishin Yu. et al. 2008; Simon et al. 2010; Zhou et al. 2012; Yoon et al. 2012; McGinn et al. 2013; Yang et al. 2013; Yi and Clark 2013; Jeong et al. 2014; Oton et al. 2015; Kim et al. 2016a; van der Asdonk et al. 2016; Peng et al. 2017b; van der Asdonk et al. 2017). Recent development of a dual-layer alignment technique to orient LCLC antiasthmatic drug, disodium cromoglycate (DSCG) (Peng et al. 2017b) allows one to photopattern complex spatially-varying structures. Since *Bacillus subtilis* may be dispersed in non-toxic DSCG (Zhou 2017), such alignment layers were able to be control the distribution, geometry and polarity of bacteria trajectories (Figure 16) (Peng et al. 2016b). Because the alignment layer and the implemented LC are both water-based, the method involves coating a protective RM layer over a preprogrammed director pattern generated by the azo-dye molecule SD1 (Peng et al. 2017b). The drawback of this method is the difficulty to assemble (uniform in thickness) LCLC cells using two glass plates with identical prepatterned director field under a polarizing optical microscope.

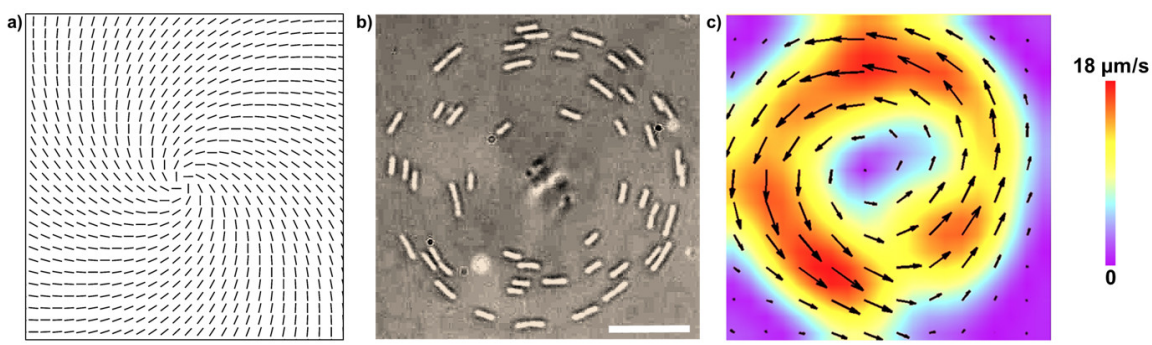

Figure 16. Unipolar circular flow of bacteria around a spiraling vortex. **a)** Prepatterned splay-bend deformations of the vortex, **b)** circular bacterial swarm enclosing the vortex center, **c)** map of bacterial velocities. Scale bar $25\ \mu m$. Peng CH, Turiv T, Guo YB, Wei QH, Lavrentovich OD (2016b) Command of active matter by topological defects and patterns. Science 354 (6314):882-885. Reprinted with permission from AAAS.

Another growing trend is to use liquid crystal based biocompatible surfaces or scaffolds for tissue growth (Agrawal et al. 2015; Kocer et al. 2017; Prevot et al. 2017; Prevot et al. 2018b; Prevot et al. 2018a). Recently, Babakhanova and colleagues developed nanogrooved surfaces (Figure 17a) using commercially available 8OCB+RM82+photoinitiator Irgacure 651 materials (Babakhanova et al. 2019). The antagonistic boundary conditions at the air/homeotropic and unidirectional planar glass interfaces induce the formation of the 'oily streak' defects in the smectic A phase (inset of Figure 17a) (Zappone and Lacaze 2008; Gharbi et al. 2017). To satisfy the anchoring, smectic layers deform into a series of hemicylinders and result in a texture that exhibits periodic light and dark linear stripes perpendicular to the easy axis (Figure 17a) (Gharbi et al. 2017). The mixture of LC reactive mesogen RM82+photoinitiator was used to

fix the molecular orientation of the defect structures in SmA phase via photopolymerization, after which the non-reactive LC was washed out.

The atomic force microscopy shows nanometer topography of the periodic 'oily streak' polymerized defect structures (Figure 17e) . When human dermal fibroblasts (hDFs) are plated on these polymerized LC nanogrooved surfaces (Figure 17d,e), the orientation of cells is guided by the topographical cues. Using the elongated nuclei of hDFs, the calculations of the orientational order parameter $(S:\ 0.75)$ show the ability to achieve highly oriented alignment of cells using LC defect structures (Figure 17b). Particularly, the cells orient their long axis predominantly parallel to the grooved direction (Figure 17d). Note that when the cells are plated onto a flat glass substrate instead, the final state of the long axis of the cells shows random orientational distribution (Figure 17b). Being able to guide cells in an orderly fashion is of extreme importance, since the cell migration plays a crucial role in chemotaxis, development, tumor invasion, immunity and tissue regeneration.

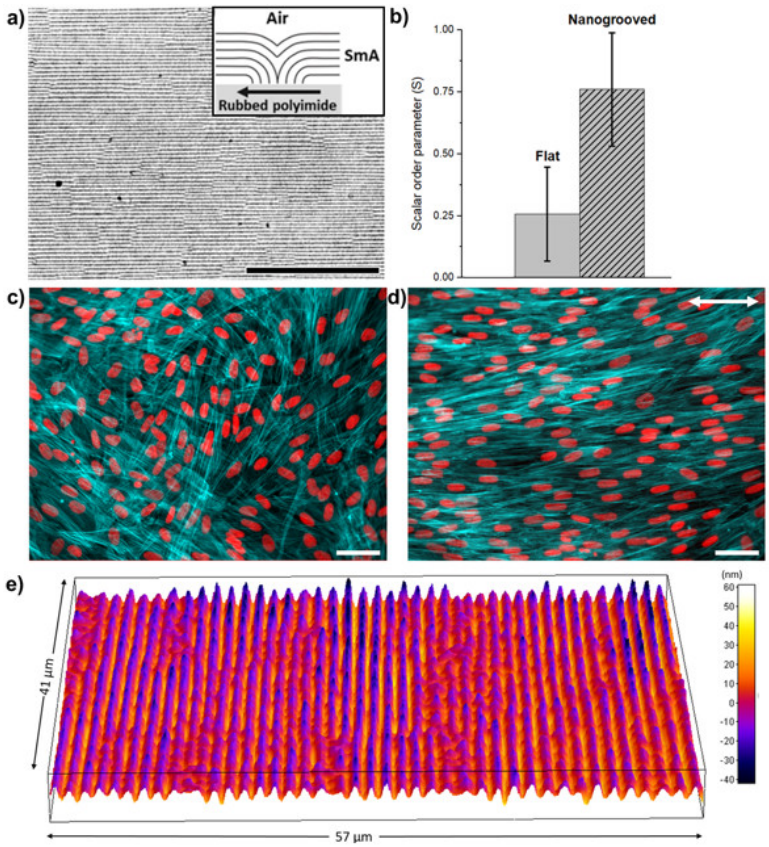

Figure 17. a) Bright field microscopy image of polymerized linear periodic SmA oily streak structures. The inset shows the formation of the oily streaks due to antagonistic boundary conditions, **b)** orientational order parameter of the elongated nuclei (illustrated in red color in panels **(c)** and **(d)**; fluorescence microscopy (Olympus IX-81) images of **c)** hDF cells oriented randomly on flat glass plate, **d)** hDF cells directed parallel to the SmA oily streak polymerized nanostructures. The arrow represents the direction of the nanogrooves, **e)** DHM image of polymerized nanogrooved surface morphology of the reactive mesogens. Scale bars $50\ \mu m$.

Conclusion and outlook

In this chapter we summarized some of the conventional methods of liquid crystal alignment. The mechanisms of planar, homeotropic and tilted alignments were briefly discussed. One of the most important aligning techniques is the photoalignment method. One may generate all three kinds of (reversible) alignment types by adjusting the conditions of the experiments. Importantly, this technique allows one to generate complex spatial patterns of the director with high accuracy. The major problem with this technique is the sensitivity of the alignment layer to environmental conditions at different stages of the preparation. Thus, there is a strong need to develop fast, inexpensive

and stable alignment methods which are not too vulnerable to processing procedures for both thermotropic and lyotropic liquid crystals. We also address the importance of developing new alignment methods for non-trivially shaped LC molecules and introduce two methods of homeotropic alignment for rigid bent-core and flexible dimeric molecules.

An important research endeavor is in the ability to generate stable alignment of LC phases (such as chiral nematic or columnar) formed by DNA/RNA molecules of different lengths/sequences, G-quartets, proteins and other biological macromolecules (Brandes and Kearns 1986; Strzelecka and Rill 1987; Strey et al. 1997; Ruckert and Otting 2000; Pfohl et al. 2001; Annila and Permi 2004; Louhivuori et al. 2006; Davis and Spada 2007; Nakata et al. 2007; Zanchetta 2009; Zanchetta et al. 2010). The ability to tailor the surface properties and roughness of the polymerizable, responsive LCs (via photoalignment for example) may be useful in ordering variety of biological macromolecules.

Another exciting and promising area of exploration involves 'active liquid crystals' composed of self-propelling units. Both, artificial and living self-propelling matter is being investigated. The ability to deterministically control the motion of particles using alignment techniques poses an interesting challenge. Lyotropic and polymerizable liquid crystal systems give rise to vast opportunities to direct biological matter (such as bacteria, cells, sperm). We presented examples of two such reports: bacteria and cell guidance. Such controllable elements may be employed as micro-machines in biomedical engineering applications. The growing trend of using polymerizable LCs are promising not only in conventional LC applications, but also in developing intelligent biomaterials with pre-programmable abilities.

Acknowledgements. The research is supported by the grant DE-SC0019105 funded by the U.S. Department of Energy, Office of Science.

References

Adlem K, Copic M, Luckhurst GR, Mertelj A, Parri O, Richardson RM, Snow BD, Timimi BA, Tuffin RP, Wilkes D (2013) Chemically induced twist-bend nematic liquid crystals, liquid crystal dimers, and negative elastic constants. Phys Rev E Stat Nonlin Soft Matter Phys 88 (2):022503. doi:10.1103/PhysRevE.88.022503

Agrawal A, Adetiba O, Kim H, Chen H, Jacot JG, Verduzco R (2015) Stimuli-responsive liquid crystal elastomers for dynamic cell culture. J Mater Res 30 (4):453-462. doi:10.1557/jmr.2014.392

Aguilar MaR, San Román J (2014) Smart polymers and their applications. Woodhead publishing in materials. Woodhead Publishing, is an imprint of Elsevier, Cambridge, UK

Aizawa M, Hisano K, Ishizu M, Akamatsu N, Barrett CJ, Shishido A (2018) Unpolarized light-induced alignment of azobenzene by scanning wave photopolymerization. Polym J 50 (8):753-759. doi:10.1038/s41428-018-0058-2

Annila A, Permi P (2004) Weakly aligned biological macromolecules in dilute aqueous liquid crystals. Concept Magn Reson A 23a (1):22-37. doi:10.1002/cmr.a.20020

Armitage D, Underwood I, Wu S-T (2006) Introduction to microdisplays. Wiley SID series in display technology. Wiley, Chichester, England ; Hoboken, NJ

Babakhanova G, Krieger J, Li B-X, Kim M-H, Lavrentovich OD (2019) Surface mediated cell alignment using polymerized liquid crystal nanostructures. [Manuscript in preparation]

Babakhanova G, Parsouzi Z, Paladugu S, Wang H, Nastishin YA, Shiyanovskii SV, Sprunt S, Lavrentovich OD (2017) Elastic and viscous properties of the nematic dimer CB7CB. Phys Rev E 96 (6):062704. doi:10.1103/PhysRevE.96.062704

Babakhanova G, Turiv T, Guo Y, Hendrikx M, Wei Q-H, Schenning APHJ, Broer DJ, Lavrentovich OD (2018) Liquid crystal elastomer coatings with programmed response of surface profile. Nat Commun 9 (1):456. doi:10.1038/s41467-018-02895-9

Bandara HMD, Burdette SC (2012) Photoisomerization in different classes of azobenzene. Chem Soc Rev 41 (5):1809-1825. doi:10.1039/c1cs15179g

Barnik M, Kozenkov V, Shtykov N, Palto S, Yudin S (1989) Photoinduced optical anisotropy in Langmuir-Blodgett films. J Mol Electron 5 (1):53-56

Berreman DW (1972) Solid Surface Shape and Alignment of an Adjacent Nematic Liquid-Crystal. Phys Rev Lett 28 (26):1683-1686. doi:DOI 10.1103/PhysRevLett.28.1683

Berreman DW (1973) Alignment of Liquid-Crystals by Grooved Surfaces. Mol Cryst Liq Cryst 23 (3-4):215-231. doi:Doi 10.1080/15421407308083374

Blinov LM (2010) Structure and properties of liquid crystals. Springer, Dordrecht Netherlands ; New York

Blinov LM, Chigrinov VG (1994) Electrooptic effects in liquid crystal materials. Partially ordered systems. Springer-Verlag, New York

Borshch V, Kim YK, Xiang J, Gao M, Jakli A, Panov VP, Vij JK, Imrie CT, Tamba MG, Mehl GH, Lavrentovich OD (2013) Nematic twist-bend phase with nanoscale modulation of molecular orientation. Nat Commun 4:2635. doi:10.1038/ncomms3635

Brake JM, Daschner MK, Luk YY, Abbott NL (2003) Biomolecular interactions at phospholipid-decorated surfaces of liquid crystals. Science 302 (5653):2094-2097. doi:DOI 10.1126/science.1091749

Brandes R, Kearns DR (1986) Magnetic ordering of DNA liquid crystals. Biochemistry-Us 25 (20):5890-5895. doi:10.1021/bi00368a008

Bushuyev OS, Aizawa M, Shishido A, Barrett CJ (2018) Shape-Shifting Azo Dye Polymers: Towards Sunlight-Driven Molecular Devices. Macromolecular Rapid Communications 39 (1):1700253. doi:10.1002/marc.201700253

Carlton RJ, Hunter JT, Miller DS, Abbasi R, Mushenheim PC, Tan LN, Abbott NL (2013) Chemical and biological sensing using liquid crystals. Liq Cryst Rev 1 (1):29-51. doi:10.1080/21680396.2013.769310

Castellano JA (1983) Surface Anchoring of Liquid-Crystal Molecules on Various Substrates. Mol Cryst Liq Cryst 94 (1-2):33-41. doi:Doi 10.1080/00268948308084245

Cestari M, Diez-Berart S, Dunmur DA, Ferrarini A, de la Fuente MR, Jackson DJB, Lopez DO, Luckhurst GR, Perez-Jubindo MA, Richardson RM, Salud J, Timimi BA, Zimmermann H (2011) Phase behavior and properties of the liquid-crystal dimer 1″,7″-bis(4-cyanobiphenyl-4′-yl) heptane: A twist-bend nematic liquid crystal. Phys Rev E 84 (3):031704. doi:10.1103/PhysRevE.84.031704

Chen D, Porada JH, Hooper JB, Klittnick A, Shen Y, Tuchband MR, Korblova E, Bedrov D, Walba DM, Glaser MA, Maclennan JE, Clark NA (2013) Chiral heliconical ground state of nanoscale pitch in a nematic liquid crystal of achiral molecular dimers. Proc Natl Acad Sci U S A 110 (40):15931-15936. doi:10.1073/pnas.1314654110

Chen J (2016) Handbook of visual display technology. Springer Berlin Heidelberg, New York, NY

Chigrinov V, Kwok HS, Takada H, Takatsu H (2005) Photo-aligning by azo-dyes: Physics and applications. Liquid Crystals Today 14 (4):1-15. doi:10.1080/14645180600617908

Chigrinov VG, Kozenkov VM, Kwok H-S (2008) Photoalignment of liquid crystalline materials : physics and applications. Wiley SID series in display technology. Wiley, Chichester, England ; Hoboken, NJ

Chrzanowski M. M. ZJ, Olifierczuk M., Kędzierski J., Nowinowski-Kruszelnicki E. (2011) Photoalignment - an alternative aligning technique for Liquid Crystal Displays. Journal of Achevements in Materials and Manufacturing Engineering 48 (1):7-13

Cognard J (1982) Alignment of Nematic Liquid-Crystals and Their Mixtures. Molecular Crystals and Liquid Crystals. Gordon and Breach Science Publishers, New York

Cognard J (1990) Lubrication with Liquid-Crystals, vol 441. Tribology and the Liquid-Crystalline State. ACS symposium series. Washington, D.C.

Cukrov G, Golestani YM, Xiang J, Nastishin YA, Ahmed Z, Welch C, Mehl GH, Lavrentovich OD (2017) Comparative analysis of anisotropic material properties of uniaxial nematics formed by flexible dimers and rod-like monomers. Liquid Crystals 44 (1):219-231. doi:10.1080/02678292.2016.1240248

Davis JT, Spada GP (2007) Supramolecular architectures generated by self-assembly of guanosine derivatives. Chem Soc Rev 36 (2):296-313. doi:10.1039/b600282j

de Gennes PG, Prost J (1995) The Physics of Liquid Crystals. 2nd ed. edn. Clarendon Press, Oxford

Dierking I (2003) Textures of liquid crystals. Wiley-VCH, Weinheim
Dyadyusha AG, Marusii TY, Reznikov YA, Khizhnyak AI, Reshetnyak VY (1992) Orientational Effect Due to a Change in the Anisotropy of the Interaction between a Liquid-Crystal and a Bounding Surface. Jetp Lett+ 56 (1):17-21
Elamain O, Hegde G, Komitov L (2013) Alignment and alignment transition of bent core nematics. Appl Phys Lett 103 (2):023301 doi:10.1063/1.4813443
Fang JY, Ma W, Selinger JV, Shashidhar R (2003) Imaging biological cells using liquid crystals. Langmuir 19 (7):2865-2869. doi:10.1021/la0264062
Fang YQ, Wang JA, Zhang Q, Zeng Y, Wang YH (2010) Synthesis of soluble polyimides for vertical alignment of liquid crystal via one-step method. Eur Polym J 46 (5):1163-1167. doi:10.1016/j.eurpolymj.2009.12.021
Fu W, Liu L, Jiang K, Li Q, Fan S (2010) Super-aligned carbon nanotube films as aligning layers and transparent electrodes for liquid crystal displays. Carbon 48 (7):1876-1879. doi:10.1016/j.carbon.2010.01.026
Fujiwara T, Ichimura K (2002) Surface-assisted photoalignment control of lyotropic liquid crystals. Part 2. Photopatterning of aqueous solutions of a water-soluble anti-asthmatic drug as lyotropic liquid crystals. Journal of Materials Chemistry 12 (12):3387-3391. doi:10.1039/b208311f
Gao K, Cheng HH, Bhowmik AK, Bos PJ (2015) Thin-film Pancharatnam lens with low f-number and high quality. Opt Express 23 (20):26086-26094. doi:10.1364/Oe.23.026086
Geary JM, Goodby JW, Kmetz AR, Patel JS (1987) The Mechanism of Polymer Alignment of Liquid-Crystal Materials. Journal of Applied Physics 62 (10):4100-4108. doi:Doi 10.1063/1.339124
Gharbi I, Missaoui A, Demaille D, Lacaze E, Rosenblatt C (2017) Persistence of Smectic-A Oily Streaks into the Nematic Phase by UV Irradiation of Reactive Mesogens. Crystals 7 (12):358. doi:10.3390/cryst7120358
Gibbons WM, Shannon PJ, Sun ST, Swetlin BJ (1991) Surface-Mediated Alignment of Nematic Liquid-Crystals with Polarized Laser-Light. Nature 351 (6321):49-50. doi:DOI 10.1038/351049a0
Guo Y, Jiang M, Peng C, Sun K, Yaroshchuk O, Lavrentovich O, Wei QH (2016) High-Resolution and High-Throughput Plasmonic Photopatterning of Complex Molecular Orientations in Liquid Crystals. Adv Mater 28 (12):2353-2358. doi:10.1002/adma.201506002
Gupta VK, Skaife JJ, Dubrovsky TB, Abbott NL (1998) Optical amplification of ligand-receptor binding using liquid crystals. Science 279 (5359):2077-2080. doi:DOI 10.1126/science.279.5359.2077
Hasegawa M (1999) Modeling of photoinduced optical anisotropy and anchoring energy of polyimide exposed to linearly polarized deep UV light. Japanese Journal of Applied Physics Part 2-Letters 38 (4b):L457-L460. doi:Doi 10.1143/Jjap.38.L457
Hecht U, Schilz CM, Stratmann M (1998) Influence of relative humidity during film formation processes on the structure of ultrathin polymeric films. Langmuir 14 (23):6743-6748. doi:DOI 10.1021/la9804987
Hiltrop K, Stegemeyer H (1978) Alignment of Liquid Crystals by Amphiphilic Monolayers. Berichte der Bunsengesellschaft für physikalische Chemie 82 (9):884-889. doi:10.1002/bbpc.19780820920
Hisano K, Aizawa M, Ishizu M, Kurata Y, Nakano W, Akamatsu N, Barrett CJ, Shishido A (2017) Scanning wave photopolymerization enables dye-free alignment patterning of liquid crystals. Science Advances 3 (11):e1701610. doi:10.1126/sciadv.1701610
Hisano K, Kurata Y, Aizawa M, Ishizu M, Sasaki T, Shishido A (2016) Alignment layer-free molecular ordering induced by masked photopolymerization with non-polarized light. Appl Phys Express 9 (7):072601. doi:10.7567/Apex.9.072601
Ho JYL, Chigrinov VG, Kwok HS (2007) Variable liquid crystal pretilt angles generated by photoalignment of a mixed polyimide alignment layer. Appl Phys Lett 90 (24):243506 doi:10.1063/1.2748345
Hunter JT, Abbott, N.L. (2012) Liquid crystals beyond displays chemistry, physics, and applications. J. Wiley & Sons, Inc., Hoboken, N.J.
Hwang JY, Lee SH, Paek SK, Seo DS (2003) Tilt angle generation for nematic liquid crystal on blended homeotropic polyimide layer containing trifluoromethyl moieties. Japanese Journal of Applied

Physics Part 1-Regular Papers Short Notes & Review Papers 42 (4a):1713-1714. doi:10.1143/Jjap.42.1713
Iadlovska OS, Maxwell GR, Babakhanova G, Mehl GH, Welch C, Shiyanovskii SV, Lavrentovich OD (2018) Tuning selective reflection of light by surface anchoring in cholesteric cells with oblique helicoidal structures. Opt Lett 43 (8):1850-1853. doi:10.1364/Ol.43.001850
Ichimura K, Fujiwara T, Momose M, Matsunaga D (2002) Surface-assisted photoalignment control of lyotropic liquid crystals. Part 1. Characterisation and photoalignment of aqueous solutions of a water-soluble dye as lyotropic liquid crystals. Journal of Materials Chemistry 12 (12):3380-3386. doi:10.1039/b208310h
Ichimura K, Suzuki Y, Seki T, Hosoki A, Aoki K (1988) Reversible Change in Alignment Mode of Nematic Liquid-Crystals Regulated Photochemically by Command Surfaces Modified with an Azobenzene Monolayer. Langmuir 4 (5):1214-1216. doi:DOI 10.1021/la00083a030
Iglesias W, Smith TJ, Basnet PB, Stefanovic SR, Tschierske C, Lacks DJ, Jakli A, Mann EK (2011) Alignment by Langmuir/Schaefer monolayers of bent-core liquid crystals. Soft Matter 7 (19):9043-9050. doi:10.1039/c1sm05546a
Jakli A, Lavrentovich OD, Selinger JV (2018) Physics of liquid crystals of bent-shaped molecules. Rev Mod Phys 90 (4):045004 doi:10.1103/RevModPhys.90.045004
Janning JL (1972) Thin-Film Surface Orientation for Liquid-Crystals. Appl Phys Lett 21 (4):173. doi:Doi 10.1063/1.1654331
Jeong JW, Han GH, Johnson ATC, Collings PJ, Lubensky TC, Yodh AG (2014) Homeotropic Alignment of Lyotropic Chromonic Liquid Crystals Using Noncovalent Interactions. Langmuir 30 (10):2914-2920. doi:10.1021/la404893t
Kahn FJ, Taylor GN, Schonhorn H (1973) Surface-Produced Alignment of Liquid-Crystals. P Ieee 61 (7):823-828. doi:Doi 10.1109/Proc.1973.9171
Kim HR, Kim JH, Kim TS, Oh SW, Choi EY (2005) Optical detection of deoxyribonucleic acid hybridization using an anchoring transition of liquid crystal alignment. Appl Phys Lett 87 (14):143901. doi:10.1063/1.2077859
Kim JB, Kim KC, Ahn HJ, Hwang BH, Kim JT, Jo SJ, Kim CS, Baik HK, Choi CJ, Jo MK, Kim YS, Park JS, Kang D (2007) No bias pi cell using a dual alignment layer with an intermediate pretilt angle. Appl Phys Lett 91 (2):023507. doi:10.1063/1.2757121
Kim JY, Nayani K, Jeong HS, Jeon HJ, Yoo HW, Lee EH, Park JO, Srinivasarao M, Jung HT (2016a) Macroscopic alignment of chromonic liquid crystals using patterned substrates. Phys Chem Chem Phys 18 (15):10362-10366. doi:10.1039/c5cp07570j
Kim YK, Breckon R, Chakraborty S, Gao M, Sprunt SN, Gleeson JT, Twieg RJ, Jakli A, Lavrentovich OD (2014a) Properties of the broad-range nematic phase of a laterally linked H-shaped liquid crystal dimer. Liquid Crystals 41 (9):1345-1355. doi:10.1080/02678292.2014.920930
Kim YK, Cukrov G, Vita F, Scharrer E, Samulski ET, Francescangeli O, Lavrentovich OD (2016b) Search for microscopic and macroscopic biaxiality in the cybotactic nematic phase of new oxadiazole bent-core mesogens. Phys Rev E 93 (6):062701. doi:10.1103/PhysRevE.93.062701
Kim YK, Cukrov G, Xiang J, Shin ST, Lavrentovich OD (2015) Domain walls and anchoring transitions mimicking nematic biaxiality in the oxadiazole bent-core liquid crystal C7. Soft Matter 11 (20):3963-3970. doi:10.1039/c5sm00580a
Kim YK, Senyuk B, Shin ST, Kohlmeier A, Mehl GH, Lavrentovich OD (2014b) Surface alignment, anchoring transitions, optical properties, and topological defects in the thermotropic nematic phase of organo-siloxane tetrapodes. Soft Matter 10 (3):500-509. doi:10.1039/c3sm52249k
Kim YK, Wang XG, Mondkar P, Bukusoglu E, Abbott NL (2018) Self-reporting and self-regulating liquid crystals. Nature 557 (7706):539. doi:10.1038/s41586-018-0098-y
Kleman M, Lavrentovich OD (2003) Soft matter physics : an introduction. Partially ordered systems. Springer, New York

Kocer G, ter Schiphorst J, Hendrikx M, Kassa HG, Leclere P, Schenning APHJ, Jonkheijm P (2017) Light-Responsive Hierarchically Structured Liquid Crystal Polymer Networks for Harnessing Cell Adhesion and Migration. Advanced Materials 29 (27):1606407. doi:10.1002/adma.201606407

Kozenkov VM, Yudin SG, Katyshev EG, Palto SP, Lazareva VT, Barachevskii VA (1986) Photoinduced Optical Anisotropy in Multilayered Langmuir Films. Pisma Zh Tekh Fiz+ 12 (20):1267-1272

Kumar A, Pattanayek SK (2016) Imaging of bacteria using chromonic liquid crystals. Mol Cryst Liq Cryst 625 (1):126-136. doi:10.1080/15421406.2015.1069441

Lakhtakia A, Messier R (2005) Sculptured thin films : nanoengineered morphology and optics. Press monograph series, vol no PM143. SPIE Press, Bellingham, Wash.

Lavrentovich OD, Ishikawa T (2002) Bulk alignment of lyotropic chromonic liquid crystals. USA Patent US6411354B1,

Lee CC (2014) The Current Trends of Optics and Photonics. Springer Netherlands,

Lee ES, Vetter P, Miyashita T, Uchida T, Kano M, Abe M, Sugawara K (1993) Control of Liquid-Crystal Alignment Using Stamped-Morphology Method. Jpn J Appl Phys 2 32 (10a):L1436-L1438. doi:Doi 10.1143/Jjap.32.L1436

Lee K-S (2003) Polymers for photonics applications II, vol 2. Nonlinear Optical, Photorefractive and Two-Photon Absorption Polymers, vol 158. Springer, Berlin

Lee KW, Lien A, Paek SH, Durning C, Fukuro H (1997) Relationship between alignment layer polymer surface structures and liquid crystal display parameters. Macromol Symp 118:505-512. doi:DOI 10.1002/masy.19971180168

Lee KW, Paek SH, Lien A, Durning C, Fukuro H (1996) Microscopic molecular reorientation of alignment layer polymer surfaces induced by rubbing and its effects on LC pretilt angles. Macromolecules 29 (27):8894-8899. doi:DOI 10.1021/ma960683w

Lee YJ, Baek JH, Kim Y, Heo JU, Yu CJ, Kim JH (2013) Enhanced surface anchoring energy for the photo-alignment layer with reactive mesogens for fast response time of liquid crystal displays. J Phys D Appl Phys 46 (14):145305. doi:10.1088/0022-3727/46/14/145305

Lee YJ, Kim YW, Du Ha J, Oh JM, Yi MH (2007) Synthesis and characterization of novel polyimides with 1-octadecyl side chains for liquid crystal alignment layers. Polym Advan Technol 18 (3):226-234. doi:10.1002/pat.862

Lee YJK, Y.K.; In, S.; Yoon, A.R.; Yu, C.J.; Kim, J.H. Liquid Crystal Alignment Control Using Reactive Mesogen Mixed with Alignment Layers. In: IDW, San Diego, CA, USA, 2009.

Li Q (2013) Intelligent stimuli-responsive materials : from well-defined nanostructures to applications. Wiley, Hoboken, New Jersey

Lin IH, Miller DS, Bertics PJ, Murphy CJ, de Pablo JJ, Abbott NL (2011) Endotoxin-Induced Structural Transformations in Liquid Crystalline Droplets. Science 332 (6035):1297-1300. doi:10.1126/science.1195639

Liou WR, Chen CY, Ho JJ, Hsu CK, Chang CC, Hsiao RY, Chang SH (2006) Improved alignment layer grown by oblique evaporation for liquid crystal devices. Displays 27 (2):69-72. doi:10.1016/j.displa.2005.11.001

Lopez DO, Robles-Hernandez B, Salud J, de la Fuente MR, Sebastian N, Diez-Berart S, Jaen X, Dunmur DA, Luckhurst GR (2016) Miscibility studies of two twist-bend nematic liquid crystal dimers with different average molecular curvatures. A comparison between experimental data and predictions of a Landau mean-field theory for the N-TB-N phase transition. Phys Chem Chem Phys 18 (6):4394-4404. doi:10.1039/c5cp07605f

Louhivuori M, Otten R, Lindorff-Larsen K, Annila A (2006) Conformational fluctuations affect protein alignment in dilute liquid crystal media. J Am Chem Soc 128 (13):4371-4376. doi:10.1021/ja0576334

Matsumori M, Takahashi A, Tomioka Y, Hikima T, Takata M, Kajitani T, Fukushima T (2015) Photoalignment of an Azobenzene-Based Chromonic Liquid Crystal Dispersed in Triacetyl Cellulose: Single-Layer Alignment Films with an Exceptionally High Order Parameter. Acs Appl Mater Inter 7 (21):11074-11078. doi:10.1021/acsami.5b02577

McCamley MK, Crawford GP, Ravnik M, Zumer S, Artenstein AW, Opal SM (2007) Optical detection of anchoring at free and fluid surfaces using a nematic liquid crystal sensor. Appl Phys Lett 91 (14):141916. doi:10.1063/1.2795347

McConney ME, Martinez A, Tondiglia VP, Lee KM, Langley D, Smalyukh II, White TJ (2013) Topography from Topology: Photoinduced Surface Features Generated in Liquid Crystal Polymer Networks. Adv Mater 25 (41):5880-5885. doi:DOI 10.1002/adma.201301891

McGinn CK, Laderman LI, Zimmermann N, Kitzerow HS, Collings PJ (2013) Planar anchoring strength and pitch measurements in achiral and chiral chromonic liquid crystals using 90-degree twist cells. Phys Rev E 88 (6):062513. doi:10.1103/PhysRevE.88.062513

Meyerhofer D (1976) New Technique of Aligning Liquid-Crystals on Surfaces. Appl Phys Lett 29 (11):691-692. doi:Doi 10.1063/1.88928

Miller DS, Wang XG, Abbott NL (2014) Design of Functional Materials Based on Liquid Crystalline Droplets. Chem Mater 26 (1):496-506. doi:10.1021/cm4025028

Murata M, Uekita M, Nakajima Y, Saitoh K (1993) Alignment of Nematic Liquid-Crystal Using Polyimide Langmuir-Blodgett Films-(Ii). Japanese Journal of Applied Physics Part 2-Letters 32 (5a):L679-L682. doi:Doi 10.1143/Jjap.32.L679

Muševič I (2017) Liquid crystal colloids. Springer Berlin Heidelberg, New York, NY

Mushenheim PC, Trivedi RR, Roy SS, Arnold MS, Weibel DB, Abbott NL (2015) Effects of confinement, surface-induced orientations and strain on dynamical behaviors of bacteria in thin liquid crystalline films. Soft Matter 11 (34):6821-6831. doi:10.1039/c5sm01489a

Mushenheim PC, Trivedi RR, Tuson HH, Weibel DB, Abbott NL (2014a) Dynamic self-assembly of motile bacteria in liquid crystals. Soft Matter 10 (1):88-95. doi:10.1039/c3sm52423j

Mushenheim PC, Trivedi RR, Weibel DB, Abbott NL (2014b) Using Liquid Crystals to Reveal How Mechanical Anisotropy Changes Interfacial Behaviors of Motile Bacteria. Biophys J 107 (1):255-265. doi:10.1016/j.bpj.2014.04.047

Nakata M, Zanchetta G, Chapman BD, Jones CD, Cross JO, Pindak R, Bellini T, Clark NA (2007) End-to-end stacking and liquid crystal condensation of 6-to 20-base pair DNA duplexes. Science 318 (5854):1276-1279. doi:10.1126/science.1143826

Nastishin Yu. A, Neupane K, Baldwin AR, Lavrentovich OD, Sprunt S (2008) Elasticity and Viscosity of a Lyotropic Chromonic Nematic Studied with Dynamic Light Scattering. eprint arXiv:08072669:arXiv:0807.2669

Ogawa T, Kanemitsu Y (1995) Optical properties of low-dimensional materials. World Scientific, Singapore ; River Edge, NJ

Oh-e M, Yokoyama H, Kim D (2004) Mapping molecular conformation and orientation of polyimide surfaces for homeotropic liquid crystal alignment by nonlinear optical spectroscopy. Phys Rev E 69 (5):051705. doi:10.1103/PhysRevE.69.051705

Oton E, Escolano JM, Quintana X, Oton JM, Geday MA (2015) Aligning lyotropic liquid crystals with silicon oxides. Liquid Crystals 42 (8):1069-1075. doi:10.1080/02678292.2015.1024767

Oton E, Lopez-Andres S, Bennis N, Oton JM, Geday MA (2014) Silicon oxides as alignment surfaces for vertically-aligned nematics in photonic devices. Opto-Electron Rev 22 (2):92-100. doi:10.2478/s11772-014-0182-2

Park H-S, Lavrentovich, O.D. (2012) Liquid crystals beyond displays chemistry, physics, and applications. John Wiley & Sons, Inc., Hoboken, New Jersey

Park JC, Park DJ, Son KC, Kim YB (2007) The properties of homeotropic alignment materials as the side chain molecular structure in polyimides. Mol Cryst Liq Cryst 479:1229-1241. doi:10.1080/15421400701734056

Pasechnik SV, Chigrinov VG, Shmeliova DV (2009) Liquid crystals : viscous and elastic properties. Wiley-VCH, Weinheim

Pelliccione M, Lu TM (2008) Evolution of thin-film morphology modeling and simulations Springer series in materials science, Berlin: Springer

Peng C, Turiv T, Guo Y, Shiyanovskii SV, Wei QH, Lavrentovich OD (2016a) Control of colloidal placement by modulated molecular orientation in nematic cells. Sci Adv 2 (9):e1600932. doi:10.1126/sciadv.1600932

Peng C, Turiv T, Zhang R, Guo Y, Shiyanovskii SV, Wei QH, de Pablo J, Lavrentovich OD (2017a) Controlling placement of nonspherical (boomerang) colloids in nematic cells with photopatterned director. J Phys Condens Matter 29 (1):014005. doi:10.1088/0953-8984/29/1/014005

Peng CH, Guo YB, Turiv T, Jiang M, Wei QH, Lavrentovich OD (2017b) Patterning of Lyotropic Chromonic Liquid Crystals by Photoalignment with Photonic Metamasks. Advanced Materials 29 (21):1606112. doi:10.1002/adma.201606112

Peng CH, Turiv T, Guo YB, Wei QH, Lavrentovich OD (2016b) Command of active matter by topological defects and patterns. Science 354 (6314):882-885. doi:10.1126/science.aah6936

Pfohl T, Kim JH, Yasa M, Miller HP, Wong GCL, Bringezu F, Wen Z, Wilson L, Kim MW, Li Y, Safinya CR (2001) Controlled modification of microstructured silicon surfaces for confinement of biological macromolecules and liquid crystals. Langmuir 17 (17):5343-5351. doi:DOI 10.1021/la010145z

Popov N, Honaker LW, Popova M, Usol'tseva N, Mann EK, Jakli A, Popov P (2018) Thermotropic Liquid Crystal-Assisted Chemical and Biological Sensors. Materials 11 (1):E20. doi:10.3390/ma11010020

Presnyakov VV, Liu ZJ, Chigrinov VG Infiltration of photonic crystal fiber with liquid crystals. In: Optics East 2005, 2005. SPIE, p 7

Prevot ME, Andro H, Alexander SLM, Ustunel S, Zhu C, Nikolov Z, Rafferty ST, Brannum MT, Kinsel B, Korley LTJ, Freeman EJ, McDonough JA, Clements RJ, Hegmann E (2018a) Liquid crystal elastomer foams with elastic properties specifically engineered as biodegradable brain tissue scaffolds. Soft Matter 14 (3):354-360. doi:10.1039/c7sm01949a

Prevot ME, Bergquist LE, Sharma A, Mori T, Gao Y, Bera T, Zhu C, Leslie MT, Cukelj R, Korley LTJ, Freeman EJ, McDonough JA, Clements RJ, Hegmann E (2017) New developments in 3D liquid crystal elastomers scaffolds for tissue engineering: from physical template to responsive substrate. Liquid Crystals Xxi 10361:103610T. doi:10.1117/12.2275338

Prevot ME, Ustunel S, Hegmann E (2018b) Liquid Crystal Elastomers-A Path to Biocompatible and Biodegradable 3D-LCE Scaffolds for Tissue Regeneration. Materials 11 (3):377. doi:10.3390/ma11030377

Rahman MDA, Agha H, Truong T-K, Park JH, Suh D, Scalia G (2018) Incorporation and orientational order of aligned carbon nanotube sheets on polymer films for liquid crystal-aligning transparent electrodes. J Mol Liq 267:363-366. doi:10.1016/j.molliq.2017.12.122

Rapini A, Papoular M (1969) Distortion d'une lamelle nématique sous champ magnétique conditions d'ancrage aux parois. J Phys Colloques 30 (C4):C4-54-C54-56

Rapp A, Ermolaev K, Fung BM (1999) The alignment of lyotropic liquid crystals formed by hexadecyltrimethylammonium bromide in D2O in a magnetic field. J Phys Chem B 103 (10):1705-1711. doi:DOI 10.1021/jp984021f

Ren Z, Lan Y, Wang Y (2013) Aligned carbon nanotubes : physics, concepts, fabrication and devices. NanoScience and technology,. Springer Verlag, Heidelberg ; New York

Roberts GG (1990) Langmuir-Blodgett films. Plenum Press, New York

Robles-Hernandez B, Sebastian N, de la Fuente MR, Lopez DO, Diez-Berart S, Salud J, Ros MB, Dunmur DA, Luckhurst GR, Timimi BA (2015) Twist, tilt, and orientational order at the nematic to twist-bend nematic phase transition of 1 ",9 "-bis(4-cyanobiphenyl-4 '-yl) nonane: A dielectric, H-2 NMR, and calorimetric study. Phys Rev E 92 (6):062505. doi:10.1103/PhysRevE.92.062505

Robles-Hernandez B, Sebastian N, Salud J, Diez-Berart S, Dunmur DA, Luckhurst GR, Lopez DO, de la Fuente MR (2016) Molecular dynamics of a binary mixture of twist-bend nematic liquid crystal dimers studied by dielectric spectroscopy. Phys Rev E 93 (6):062705. doi:10.1103/PhysRevE.93.062705

Ruckert M, Otting G (2000) Alignment of biological macromolecules in novel nonionic liquid crystalline media for NMR experiments. J Am Chem Soc 122 (32):7793-7797. doi:10.1021/ja001068h

Ruslim C, Hashimoto M, Matsunaga D, Tamaki T, Ichimura K (2004) Optical and surface morphological properties of polarizing films fabricated from a chromonic dye by the photoalignment technique. Langmuir 20 (1):95-100. doi:10.1021/la035366e

Russell JM, Oh SJ, LaRue I, Zhou O, Samulski ET (2006) Alignment of nematic liquid crystals using carbon nanotube films. Thin Solid Films 509 (1-2):53-57. doi:10.1016/j.tsf.2005.09.099

Schadt M (2017) Liquid crystal displays, LC-materials and LPP photo-alignment. Mol Cryst Liq Cryst 647 (1):253-268. doi:10.1080/15421406.2017.1289604

Schadt M, Schmitt K, Kozinkov V, Chigrinov V (1992) Surface-Induced Parallel Alignment of Liquid-Crystals by Linearly Polymerized Photopolymers. Japanese Journal of Applied Physics Part 1-Regular Papers Short Notes & Review Papers 31 (7):2155-2164. doi:Doi 10.1143/Jjap.31.2155

Sebastian N, Robles-Hernandezb B, Diez-Berart S, Saludc J, Luckhurst GR, Dunmur DA, Lopez DO, La Fuente MR (2017) Distinctive dielectric properties of nematic liquid crystal dimers. Liquid Crystals 44 (1):177-190. doi:10.1080/02678292.2016.1218963

Sebastian N, Tamba MG, Stannarius R, de la Fuente MR, Salamonczyk M, Cukrov G, Gleeson J, Sprunt S, Jakli A, Welch C, Ahmed Z, Mehl GH, Eremin A (2016) Mesophase structure and behaviour in bulk and restricted geometry of a dimeric compound exhibiting a nematic-nematic transition. Phys Chem Chem Phys 18 (28):19299-19308. doi:10.1039/c6cp03899a

Senyuk B, Kim YK, Tortora L, Shin ST, Shiyanovskii SV, Lavrentovich OD (2011) Surface Alignment, Anchoring Transitions, Optical Properties and Topological Defects in Nematic Bent-Core Materials C7 and C12. Mol Cryst Liq Cryst 540:20-41. doi:10.1080/15421406.2011.568324

Senyuk B, Wonderly H, Mathews M, Li Q, Shiyanovskii SV, Lavrentovich OD (2010) Surface alignment, anchoring transitions, optical properties, and topological defects in the nematic phase of thermotropic bent-core liquid crystal A131. Phys Rev E 82 (4):041711. doi:10.1103/PhysRevE.82.041711

Shiyanovskii SV, Schneider T, Smalyukh II, Ishikawa T, Niehaus GD, Doane KJ, Woolverton CJ, Lavrentovich OD (2005) Real-time microbe detection based on director distortions around growing immune complexes in lyotropic chromonic liquid crystals. Phys Rev E 71 (2):020702. doi:10.1103/PhysRevE.71.020702

Shteyner EA, Srivastava AK, Chigrinov VG, Kwok HS, Afanasyev AD (2013) Submicron-scale liquid crystal photo-alignment. Soft Matter 9 (21):5160-5165. doi:10.1039/c3sm50498k

Simon KA, Burton EA, Cheng F, Varghese N, Falcone ER, Wu L, Luk YY (2010) Controlling Thread Assemblies of Pharmaceutical Compounds in Liquid Crystal Phase by Using Functionalized Nanotopography. Chem Mater 22 (8):2434-2441. doi:10.1021/cm901477a

Skarp K, Matuszczyk M, Matuszczyk T, Bijlenga B, Hornell A, Stebler B, Lagerwall ST (1988) A 1″ × 0.5″ FLC bar-graph display with short-term memory. Ferroelectrics 85:313-325

Slussarenko S, Murauski A, Du T, Chigrinov V, Marrucci L, Santamato E (2011) Tunable liquid crystal q-plates with arbitrary topological charge. Opt Express 19 (5):4085-4090. doi:Doi 10.1364/Oe.19.004085

Son I, Kim JH, Lee B, Kim C, Yoo JY, Cho CH, Lee JH (2017) Stabilization of in situ self-assembled homeotropic alignment layer for liquid crystals by photopolymerization of reactive monomer. Mol Cryst Liq Cryst 654 (1):6-11. doi:10.1080/15421406.2017.1354665

Strey HH, Parsegian VA, Podgornik R (1997) Equation of state for DNA liquid crystals: Fluctuation enhanced electrostatic double layer repulsion. Phys Rev Lett 78 (5):895-898. doi:DOI 10.1103/PhysRevLett.78.895

Strzelecka TE, Rill RL (1987) Solid-State P-31 Nmr-Studies of DNA Liquid-Crystalline Phases - the Isotropic to Cholesteric Transition. J Am Chem Soc 109 (15):4513-4518. doi:DOI 10.1021/ja00249a014

Sung SJ, Kim HT, Lee JW, Park JK (2001) Photo-induced liquid crystal alignment on polyimide containing fluorine group. Synthetic Met 117 (1-3):277-279. doi:Doi 10.1016/S0379-6779(00)00385-4

Takatoh K (2005) Alignment technologies and applications of liquid crystal devices Liquid crystals book series

Theis JG, Smith GP, Yi Y, Walba DM, Clark NA (2018) Liquid crystal phase behavior of a DNA dodecamer and the chromonic dye Sunset Yellow. Phys Rev E 98 (4):042701. doi:10.1103/PhysRevE.98.042701

Toney MF, Russell TP, Logan JA, Kikuchi H, Sands JM, Kumar SK (1995) Near-Surface Alignment of Polymers in Rubbed Films. Nature 374 (6524):709-711. doi:DOI 10.1038/374709a0

Truong T-K, Park JH, Rahman MDA, Urbanski M, Kim ES, Scalia G, Suh D (2019) Dynamic operation of liquid crystal cell with inherently nanogroove-featured aligned carbon nanotube sheets. Current Applied Physics 19 (2):162-167. doi:10.1016/j.cap.2018.11.018

van Aerle NAJM, Tol AJW (1994) Molecular-Orientation in Rubbed Polyimide Alignment Layers Used for Liquid-Crystal Displays. Macromolecules 27 (22):6520-6526. doi:DOI 10.1021/ma00100a042

van der Asdonk P, Collings PJ, Kouwer PHJ (2017) Fully Stable and Homogeneous Lyotropic Liquid Crystal Alignment on Anisotropic Surfaces. Adv Funct Mater 27 (28):1701209. doi: 10.1002/adfm.201701209

van der Asdonk P, Hendrikse HC, Romera MFC, Voerman D, Ramakers BEI, Lowik DWPM, Sijbesma RP, Kouwer PHJ (2016) Patterning of Soft Matter across Multiple Length Scales. Adv Funct Mater 26 (16):2609-2616. doi:10.1002/adfm.201504945

Vanaerle NAJM, Barmentlo M, Hollering RWJ (1993) Effect of Rubbing on the Molecular-Orientation within Polyimide Orienting Layers of Liquid-Crystal Displays. Journal of Applied Physics 74 (5):3111-3120. doi:Doi 10.1063/1.354577

Vaughn KE, Sousa M, Kang D, Rosenblatt C (2007) Continuous control of liquid crystal pretilt angle from homeotropic to planar. Appl Phys Lett 90 (19):194102. doi:10.1063/1.2737427

Wai Tam AM, Fan F, Chen H-S, Du T, Chigrinov VG, Lin Y-H, Kwok H-S (2016) 44-3: Nanoscopic Patterned Photo-alignment for Electrically Switchable Liquid Crystal Pancharatnam-Berry Phase Diffractive Lens. SID Symposium Digest of Technical Papers 47 (1):599-601. doi:10.1002/sdtp.10751

Wang JR, McGinty C, West J, Bryant D, Finnemeyer V, Reich R, Berry S, Clark H, Yaroshchuk O, Bos P (2017) Effects of humidity and surface on photoalignment of brilliant yellow. Liquid Crystals 44 (5):863-872. doi:10.1080/02678292.2016.1247479

Wang YH, Xu CY, Kanazawa A, Shiono T, Ikeda T, Matsuki Y, Takeuchi Y (2001) Thermal stability of alignment of a nematic liquid crystal induced by polyimides exposed to linearly polarized light. Liquid Crystals 28 (3):473-475. doi:Doi 10.1080/02678290010017962

Ware TH, McConney ME, Wie JJ, Tondiglia VP, White TJ (2015) Voxelated liquid crystal elastomers. Science 347 (6225):982-984. doi:10.1126/science.1261019

White TJ, Broer DJ (2015) Programmable and adaptive mechanics with liquid crystal polymer networks and elastomers. Nat Mater 14 (11):1087-1098. doi:10.1038/Nmat4433

Woolverton CJ, Gustely E, Li L, Lavrentovich OD (2005) Liquid crystal effects on bacterial viability. Liquid Crystals 32 (4):417-423. doi:10.1080/02678290500074822

Wu WY, Wang CC, Fuh AYG (2008) Controlling pre-tilt angles of liquid crystal using mixed polyimide alignment layer. Opt Express 16 (21):17131-17137. doi:Doi 10.1364/Oe.16.017131

Xiang J, Li Y, Li Q, Paterson DA, Storey JM, Imrie CT, Lavrentovich OD (2015) Electrically tunable selective reflection of light from ultraviolet to visible and infrared by heliconical cholesterics. Advanced Materials 27 (19):3014-3018. doi:10.1002/adma.201500340

Xiang J, Shiyanovskii SV, Imrie CT, Lavrentovich OD (2014a) Electrooptic Response of Chiral Nematic Liquid Crystals with Oblique Helicoidal Director. Phys Rev Lett 112 (21):217801. doi:10.1103/PhysRevLett.112.217801

Xiang J, Shiyanovskii SV, Li YN, Imrie CT, Li Q, Lavrentovich OD (2014b) Electrooptics of chiral nematics formed by molecular dimers. Liquid Crystals Xviii 9182:91820P-91821 – 91820P-91829. doi:10.1117/12.2062737

Yang D-K, Wu S-T (2014) Fundamentals of liquid crystal devices. Wiley series in display technology, Second edition. edn. John Wiley & Sons Inc., Chichester, West Sussex, United Kingdom

Yang D-K, Wu S-T (2015) Fundamentals of liquid crystal devices. Wiley series in display technology, Second edition. edn. Wiley, Chichester, West Sussex, United Kingdom

Yang KH, Tajima K, Takenaka A, Takano H (1996) Charge trapping properties of uv-exposed polyimide films for the alignment of liquid crystals. Jpn J Appl Phys 2 35 (5a):L561-L563. doi:Doi 10.1143/Jjap.35.L561

Yang SJ, Wang B, Cui DW, Kerwood D, Wilkens S, Han JJ, Luk YY (2013) Stereochemical Control of Nonamphiphilic Lyotropic Liquid Crystals: Chiral Nematic Phase of Assemblies Separated by Six Nanometers of Aqueous Solvents. J Phys Chem B 117 (23):7133-7143. doi:10.1021/jp401382h

Yaroshchuk O, Reznikov Y (2012) Photoalignment of liquid crystals: basics and current trends. Journal of Materials Chemistry 22 (2):286-300. doi:10.1039/c1jm13485j

Yeung FS, Ho JY, Li YW, Xie FC, Tsui OK, Sheng P, Kwok HS (2006a) Variable liquid crystal pretilt angles by nanostructured surfaces. Appl Phys Lett 88 (5):051910. doi:10.1063/1.2171491

Yeung FSY, Xie FC, Wan JTK, Lee FK, Tsui OKC, Sheng P, Kwok HS (2006b) Liquid crystal pretilt angle control using nanotextured surfaces. Journal of Applied Physics 99 (12):124506. doi:10.1063/1.2206067

Yi Y, Clark NA (2013) Orientation of chromonic liquid crystals by topographic linear channels: multi-stable alignment and tactoid structure. Liquid Crystals 40 (12):1736-1747. doi:10.1080/02678292.2013.839831

Yoon DK, Smith GP, Tsai E, Moran M, Walba DM, Bellini T, Smalyukh II, Clark NA (2012) Alignment of the columnar liquid crystal phase of nano-DNA by confinement in channels. Liquid Crystals 39 (5):571-577. doi:10.1080/02678292.2012.666809

Yoon H, Kang SW, Lehmann M, Park JO, Srinivasarao M, Kumar S (2011) Homogeneous and homeotropic alignment of bent-core uniaxial and biaxial nematic liquid crystals. Soft Matter 7 (19):8770-8775. doi:10.1039/c1sm05653k

Yun C-J, Vengatesan MR, Vij JK, Song J-K (2015) Hierarchical elasticity of bimesogenic liquid crystals with twist-bend nematic phase. Appl Phys Lett 106 (17):173102. doi:10.1063/1.4919065

Zanchetta G (2009) Spontaneous self-assembly of nucleic acids: liquid crystal condensation of complementary sequences in mixtures of DNA and RNA oligomers. Liquid Crystals Today 18 (2):40-49. doi:10.1080/13583140903155093

Zanchetta G, Giavazzi F, Nakata M, Buscaglia M, Cerbino R, Clark NA, Bellini T (2010) Right-handed double-helix ultrashort DNA yields chiral nematic phases with both right- and left-handed director twist. P Natl Acad Sci USA 107 (41):17497-17502. doi:10.1073/pnas.1011199107

Zappone B, Lacaze E (2008) Surface-frustrated periodic textures of smectic-A liquid crystals on crystalline surfaces. Phys Rev E 78 (6):061704. doi:10.1103/PhysRevE.78.061704

Zhou S (2017) Lyotropic chromonic liquid crystals. Springer Berlin Heidelberg, New York, NY

Zhou S, Nastishin YA, Omelchenko MM, Tortora L, Nazarenko VG, Boiko OP, Ostapenko T, Hu T, Almasan CC, Sprunt SN, Gleeson JT, Lavrentovich OD (2012) Elasticity of Lyotropic Chromonic Liquid Crystals Probed by Director Reorientation in a Magnetic Field. Phys Rev Lett 109 (3):037801. doi:10.1103/PhysRevLett.109.037801

Zhou S, Sokolov A, Lavrentovich OD, Aranson IS (2014) Living liquid crystals. P Natl Acad Sci USA 111 (4):1265-1270. doi:10.1073/pnas.1321926111

Zhou S, Tovkach O, Golovaty D, Sokolov A, Aranson IS, Lavrentovich OD (2017) Dynamic states of swimming bacteria in a nematic liquid crystal cell with homeotropic alignment. New J Phys 19:055006. doi:10.1088/1367-2630/aa695b

Zhu YM, Wang L, Lu ZH, Wei Y, Chen XX, Tang JH (1994) Atomic-Force Microscopic Study of Rubbed Polyimide Films. Appl Phys Lett 65 (1):49-51. doi:Doi 10.1063/1.113069